

Self-Consistent Field Calculations for the Effect of Pressure and Temperature on Some Properties of Grey Tin Crystal

**A Thesis
Submitted to the Council of the College of Science
University of Babylon
In Partial Fulfillment of the Requirements for the
Degree of Master of Science in Physics**

**By
Mohammad Ghanim Merdan**



December - ٢٠٠٥

حسابات المجال المتوافق ذاتياً لتأثير الضغط ودرجة الحرارة في بعض خواص بلورة القصدير الرمادي

رسالة مقدمة إلى
مجلس كلية العلوم - جامعة بابل
وهي جزء من متطلبات نيل درجة ماجستير علوم
في علوم الفيزياء

من قبل
محمد غانم مردان



شوال ١٤٢٦

كانون الأول ٢٠٠٥

الخلاصة

استعملت طريقة خلية الوحدة الكبيرة (LUC) بثماني ذرات مع تقريب الإهمال المتوسط للتداخل التفاضلي (INDO) لدراسة بعض خواص بلورة القصدير الرمادي، ($\alpha - \text{Sn}$) ولدراسة تأثير الضغط ودرجة الحرارة في هذه الخواص. تمت إضافة تصحيحات الترابط مع الأخذ بالحسبان الانشطار البرمي المداري. تم الحصول على كل من طاقة الترابط وفجوة الطاقة المباشرة و عرض حزمة التكافؤ و عرض حزمة التوصيل والمدارات المهجنة للبلورة من خلال حسابات التركيب الحزمي. وكذلك تم حساب معامل المرونة الحجمي، توزيع شحنة التكافؤ وعامل تشكيل الأشعة السينية. تم الحصول على الخواص المذكورة باختيار مجموعة معلمات شبيهة تجريبية لنموذج (LUC-INDO). وقد وجد أن ثابت الشبكة عن نقطة التوازن وطاقة الترابط وعامل تشكيل الأشعة السينية في توافق جيد مع القيم العملية بينما كانت قيمة فجوة الطاقة ومعامل المرونة الحجمي اكبر من القيم العملية.

وقد درس تأثير اجهاد كبس في الخواص المذكورة سابقاً ووجد أن فجوة الطاقة و عرض حزمة التكافؤ واشغال الحالة p تزداد مع زيادة اجهاد كبس، بينما يحصل نقصان في عرض حزمة التوصيل وعامل تشكيل الأشعة السينية. وقد وجد أن تصرف هذه الخواص معاكس لتصرفها مع اجهاد سحب. اعتمدت أعلى قيمة للاجهد لتكون (1 GPa) لأن القصدير يتحول من طور ($\alpha - \text{Sn}$) إلى طور ($\beta - \text{Sn}$) عند هذه القيمة من الاجهاد تقريباً.

تمت دراسة تأثير الحرارة في الخواص المذكورة سابقاً. إن تأثير الحرارة في هذا العمل يمثل التغير في الخواص الناتج من تغير ثابت الشبكة للبلورة مع تغير درجة الحرارة. وقد وجد أن عرض حزمة التوصيل واشغال الحالة s وعامل تشكيل الأشعة السينية تزداد مع زيادة درجة الحرارة، في حين يحصل نقصان في فجوة الطاقة و عرض حزمة التكافؤ. وقد درس تأثير درجة الحرارة بمدى لا يتجاوز 13.2°C بسبب انتقال القصدير من الطور ($\alpha - \text{Sn}$) إلى الطور ($\beta - \text{Sn}$) عند هذه الدرجة.

استنتج من هذا العمل إن أنموذج LUC-INDO يعطي نتائج جيدة فيما إذا تم اختيار قيم مثلى للعوامل شبيهة التجريبية، ويمكن أن يعطي توقعاً جيداً لتأثير الضغط. ولدراسة تأثير الحرارة بشكل كامل، فإن إضافة الإسهام الاهتزازي للطاقة يعد ضرورياً.

LIST OF FIGURES

No.	The Title	Pages
3.8	Lattice constant of $(\alpha - \text{Sn})$ as a function of compressive stress	69
3.9	Lattice constant of $(\alpha - \text{Sn})$ as a function of tensile stress	69
3.10	Effect of compressive stress on the cohesive energy of $(\alpha - \text{Sn})$	70
3.11	Effect of tensile stress on the cohesive energy of $(\alpha - \text{Sn})$	71
3.12	Effect of compressive stress on the conduction band width of $(\alpha - \text{Sn})$	72
3.13	Effect of compressive stress on the band gap width of $(\alpha - \text{Sn})$	73
3.14	Effect of compressive stress on the valence band width of $(\alpha - \text{Sn})$	73
3.15	Effect of tensile stress on the conduction band width of $(\alpha - \text{Sn})$	74
3.16	Effect of tensile stress on the band gap width of $(\alpha - \text{Sn})$	74
3.17	Effect of tensile stress on the valence band width of $(\alpha - \text{Sn})$	75
3.18	Effect of compressive stress on the energy of Γ_1	75
3.19	Effect of compressive stress on the energy of Γ_2	76
3.20	Effect of compressive stress on the energy of X_{1v}	76
3.21	Effect of compressive stress on the energy of X_{1v}	77
3.22	Effect of compressive stress on the energy of X_{1c}	77
3.23	Effect of compressive stress on the energy of X_{1c}	78
3.24	Effect of tensile stress on the energy of Γ_1	78
3.25	Effect of tensile stress on the energy of Γ_2	79
3.26	Effect of tensile stress on the energy of X_{1v}	79

LIST OF FIGURES

No.	The Title	Pages
३.२७	Effect of tensile stress on the energy of x_{ξ_v}	१०
३.२८	Effect of tensile stress on the energy of x_{ξ_c}	१०
३.२९	Effect of tensile stress on the energy of x_{ξ_c}	११
३.३०	Valence charge density of $(\alpha-Sn)$ in the $(\bar{y}\bar{0}\bar{0})$ plane at compressive stress of १GPa	१३
३.३१	Valence charge density of $(\alpha-Sn)$ in the $(\bar{0}\bar{0}\bar{1})$ plane at compressive stress of १GPa	१०
३.३२	Valence charge density of $(\alpha-Sn)$ in the $(\bar{z}\bar{0}\bar{0})$ plane at compressive stress of १GPa	१०
३.३३	Valence charge density of $(\alpha-Sn)$ in the $(\bar{y}\bar{0}\bar{0})$ plane at tensile stress of -१GPa	१६
३.३३	Valence charge density of $(\alpha-Sn)$ in the $(\bar{0}\bar{0}\bar{1})$ plane at tensile stress of -१GPa	१६
३.३०	Valence charge density of $(\alpha-Sn)$ in the $(\bar{z}\bar{0}\bar{0})$ plane at tensile stress of -१GPa	१७
३.३६	The linear thermal expansion coefficient of tin as a function of temperature	१०
३.३७	The lattice constant of tin as a function of temperature	१०
३.३८	Cohesive energy of $(\alpha-Sn)$ as a function of temperature	११
३.३९	Effect of temperature on the conduction band width of $(\alpha-Sn)$	१२
३.३०	Effect of temperature on the band gap width of $(\alpha-Sn)$	१३
३.३१	Effect of temperature on the valence band width of $(\alpha-Sn)$	१३

LIST OF FIGURES

No.	The Title	Pages
۳.۴۲	Effect of temperature on the energy of Γ_v	۹۴
۳.۴۳	Effect of temperature on the energy of Γ_v	۹۴
۳.۴۴	Effect of temperature on the energy of X_{1v}	۹۵
۳.۴۵	Effect of temperature on the energy of $X_{\epsilon v}$	۹۵
۳.۴۶	Effect of temperature on the energy of X_{1c}	۹۶
۳.۴۷	Effect of temperature on the energy of $X_{\epsilon c}$	۹۶
۳.۴۸	Valence charge density of $(\alpha-Sn)$ in the $(\bar{2}00)$ plane at temperature of $(\bar{2}80\text{ K})$	۹۸
۳.۴۹	Valence charge density of $(\alpha-Sn)$ in the $(00\bar{1})$ plane at temperature of $(\bar{2}80\text{ K})$	۹۸
۳.۵۰	Valence charge density of $(\alpha-Sn)$ in $(\bar{1}00)$ plane at temperature of $(\bar{2}80\text{ K})$	۹۹

Abstract

A large unit cell (LUC) formalism of eight atoms within intermediate neglect of differential overlap (INDO) is used to study some properties of grey tin crystal and to investigate the effect of pressure and temperature on these properties. Correlation corrections are added to this model and taking the spin-orbit splitting into consideration. Cohesive energy, direct band gap, valence band width, conduction band width and hybridized orbitals of the crystal are obtained from the band structure calculations. Bulk modulus, valence charge distribution and x-ray scattering factors are also calculated. All the aforementioned properties are obtained by selecting empirical parameter sets for (LUC-INDO) model. It is found that the equilibrium lattice constant, cohesive energy, x-ray scattering factors are in good agreement with the experimental results. The direct band gap and bulk modulus are greater than the experimental values.

The effect of compressive stress on the aforementioned properties is investigated. It is found that the direct band gap, valence band width and p state occupation increase with increasing the compressive stress, whereas the conduction band width and form factors decrease. The reverse of these behaviours are found with the effect of tensile stress. The maximum value of stress is taken to be 1 GPa, because at this value α -Sn transforms to β -Sn.

The effect of temperature on these properties is studied below 13.2°C because beyond this value α -Sn has phase transition to β -Sn. The effect of temperature in the present work represents the change of the properties due to the change in the lattice constant of the crystal. It is found that the conduction band width, s state occupation and form factors increase with increasing the temperature, while the direct band gap and valence band width decrease.

It is concluded that the (LUC-INDO) method gives good results when choosing optimum empirical parameter sets and it has a reliable prediction for the effect of pressure. This model is deficient for the effect of temperature because the adding of the vibrational contribution to free energy of the crystal is necessary.

CONTENTS

No.	Subjects	Pages
२.६	The Hartree Approximation	२१
२.७	The Hartree-Fock Approximation	२२
२.८	The Energy Expression for a Closed Shell System	२६
२.९	Hartree-Fock Equations	२७
२.१०	Self-Consistent Field Theory (SCF)	२९
२.११	Linear Combination of Atomic Orbitals (LCAO)	२९
२.१२	Basis Sets	३०
२.१२.१	Slater-Type Orbitals (STO)	३२
२.१२.२	Gaussian-Type Orbitals (GTO)	३२
२.१३	Roothaan-Hall Equations	३३
२.१४	Semi-empirical Methods	३६
२.१४.१	Complete Neglect of Differential Overlap (CNDO) ...	३७
२.१४.२	Intermediate Neglect of Differential Overlap (INDO) ..	४०
२.१५	Tight-Binding Method (TBM)	४१
२.१६	The Large Unit Cell-INDO Method	४७
२.१७	Corrections to the Hartree-Fock Theory	४७
२.१७.१	Correlation Corrections	४७
२.१७.२	Relativistic Corrections	५०
Chapter ३ Computations and Results		
३.१	The Structure of Computer Program	५२

CONTENTS

No.	Subjects	Pages
३.२	Choice of Large Unit Cell	०६
३.३	Choice of Parameters	००
३.६	The Total Energy	०६
३.०	The Cohesive Energy	०८
३.६	Band Structure	०९
३.१	Valance Electronic Charge Densities	६२
३.८	Bulk Modulus	६६
३.९	X-Ray Scattering Factor	६६
३.१०	Determination of the Lattice Constant as a function of Pressure ..	६१
३.११	Effect of Pressure on the Band Structure and Some Physical Properties of the Grey Tin Crystal	१०
३.११.१	Cohesive Energy	१०
३.११.२	Band Structure	११
३.११.३	Hybridization State	८१
३.११.६	Valance Electronic Charge Densities	८६
३.११.०	X-Ray Scattering Factors	८१
३.१२	Determination of the Lattice Constant as a Function of Temperature	८९
३.१३	Effect of Temperature on the Band Structure and Some Physical Properties of Grey Tin Crystal	९१
३.१३.१	Cohesive Energy	९१
३.१३.२	Band Structure	९२

CONTENTS

No.	Subjects	Pages
۳.۱۳.۳	Hybridization State	۹۷
۳.۱۳.۳	Hybridization State	۹۷
۳.۱۳.۴	Valence Electronic Charge Densities	۹۷
۳.۱۳.۵	X-Ray Scattering Factors	۹۹
Chapter ۴ Discussion, Conclusions and Suggestions		
۴.۱	Discussion of the Results	۱۰۱
۴.۱.۱	The Empirical Parameters	۱۰۱
۴.۱.۲	The Total Energy	۱۰۲
۴.۱.۳	The Cohesive Energy	۱۰۲
۴.۱.۴	The Direct Band Gap	۱۰۳
۴.۱.۵	The Valence and Conduction Band Width	۱۰۴
۴.۱.۶	Hybrid Crystal Orbitals	۱۰۵
۴.۱.۷	The Bulk Modulus	۱۰۵
۴.۱.۸	Valence Charge Distribution	۱۰۶
۴.۱.۹	X-Ray Scattering Factors	۱۰۷
۴.۲	Conclusions	۱۰۸
۴.۳	Suggestions	۱۱۰
	References	۱۱۲
	Appendix A: The Overlap Integrals and Slater Integrals	۱۱۹
	Appendix B: Two-Center and One-Center Coulomb Integrals in INDO Approximation	۱۲۳

CONTENTS

LIST OF TABLES

No.	The Title	Pages
۳.۷	Calculated atomic form factors of (α -Sn) crystal in comparison with experiments and previous HF calculations	۶۷
۳.۸	Effect of compressive stress on the hybridization state	۸۲
۳.۹	Effect of tensile stress on the hybridization state	۸۳
۳.۱۰	Effect of compressive stress on the form factors of (α -Sn)	۸۸
۳.۱۱	Effect of tensile stress on the form factors of (α -Sn)	۸۸
۳.۱۲	Effect of temperature on the hybridization state	۹۷
۳.۱۳	Effect of temperature on x-ray scattering factors	۱۰۰

Table (3.13): Effect of temperature on x-ray scattering factors

Reflection (hkl)	X-ray scattering factors										
	Temperature (K)										
	1.	3.	6.	9.	12.	15.	18.	21.	24.	27.	280
(111)	44.407	44.408	44.473	44.479	44.473	44.478	44.484	44.490	44.497	44.503	44.500
(220)	39.077	39.078	39.087	39.093	39.701	39.708	39.717	39.720	39.734	39.744	39.748
(311)	37.443	37.440	37.453	37.472	37.470	37.479	37.488	37.498	37.509	37.520	37.524
(400)	30.371	30.374	30.383	30.392	30.401	30.411	30.421	30.432	30.443	30.450	30.459
(331)	33.031	33.034	33.044	33.056	33.077	33.078	33.090	33.103	33.117	33.131	33.137
(422)	30.737	30.739	30.751	30.764	30.777	30.789	30.703	30.717	30.733	30.750	30.750
(011)	30.342	30.340	30.357	30.379	30.380	30.392	30.400	30.419	30.434	30.450	30.450
(333)	29.423	29.427	29.438	29.451	29.473	29.477	29.490	29.500	29.520	29.537	29.543

APPENDIX A. THE OVERLAP INTEGRALS AND SLATER INTEGRALS

$$T(\mu, \nu) = D(l_a, l_b, m) \sum_{\mu}^{l_a-m} \sum_{\nu}^{l_b-m} C_{l_a, \mu} C_{l_b, \nu} (\mu^2 - 1)^m \times (1 - \nu^2)^m \quad (\text{A.}\circ)$$

$$(1 + \mu\nu)^u (1 - \mu\nu)^v (\mu + \nu)^{-m-u} (\mu - \nu)^{-m-v}$$

Where

$$D(l_a, l_b, m) = \left(\frac{(m+1)!}{8} \right)^2 \left(\frac{2l_a + 1}{2} \frac{(l_a - m)!}{(l_a + m)!} \right)^{\frac{1}{2}} \quad (\text{A.}\uparrow)$$

$$\times \left(\frac{2l_b + 1}{2} \frac{(l_b - m)!}{(l_b + m)!} \right)^{\frac{1}{2}}$$

All the two center integrals reduced to expressions involving one or more basic two-center integrals are known as the reduced overlap integral which is given as

$$s(n_a, l_a, m, n_b, l_b, \alpha, \beta) = \int_{-1}^{\infty} \int_{-1}^1 (\mu + \nu)^{n_a} (\mu - \nu)^{n_b} \quad (\text{A.}\uparrow)$$

$$\times \exp[-\frac{1}{2}(\alpha + \beta)\mu - \frac{1}{2}(\alpha - \beta)\nu] T(\mu, \nu) d\mu d\nu$$

Where n_a and n_b are the principal quantum number for a and b respectively. Substituting Eq. (A.○) into Eq. (A.↑) and using the formula that given for l_a . l_b and m.

$$\sum_{\mu}^{l_a-m} \sum_{\nu}^{l_b-m} C_{l_a, \mu} C_{l_b, \nu} (\mu^2 - 1)^m (1 - \nu^2)^m (1 + \mu\nu)^u (1 - \mu\nu)^v \quad (\text{A.}\wedge)$$

$$\times (\mu + \nu)^{n_a - m - \mu} (\mu - \nu)^{n_b - m - \nu} = \sum_{i,j=0} Y_{ij\lambda} \mu^i \nu^j$$

Where λ is a function of n_a , n_b , l_a , l_b and m. $C_{l, \mu}$ is defined in the section (V.1○).

The reduced overlap integral can be written as

APPENDIX A. THE OVERLAP INTEGRALS AND SLATER INTEGRALS

$$s(n_a, l_a, m, n_b, l_b, \alpha, \beta) = D(l_a, l_b, m) \sum_{ij} Y_{ij\lambda} A_i \left[\frac{1}{2}(\alpha + \beta) \right] B_j \times \left[\frac{1}{2}(\alpha - \beta) \right] \quad (\text{A. } 9)$$

Where A_i and B_j are the auxiliary functions which are given as,

$$A_i(\rho) = \int_1^{\infty} X^i \exp(-\rho X) dx = \exp(-\rho) \sum_{\mu=1}^{i+1} \frac{i!}{\rho^\mu (i - \mu + 1)!} \quad (\text{A. } 10)$$

$$B_j(\rho) = \int_{-1}^1 X^j \exp(-\rho X) dx = -\exp(-\rho) \sum_{\mu=1}^{j+1} \frac{j!}{\rho^\mu (j - \mu + 1)!} - \exp(-\rho) \sum_{\mu=1}^{j+1} \frac{(-1)^{j-\mu} j!}{\rho^\mu (j - \mu + 1)!} \quad (\text{A. } 11)$$

Eq. (A. 9) is programmed in this form as a subroutine used in this work.

Now, the overlap integral can be evaluated as,

$$S_{ab} = \int \Omega_{ab}(1) d\tau \quad (\text{A. } 12)$$

Where Ω_{ab} is a product of any two Slater functions, ϕ_a and ϕ_b ,

$$\Omega_{ab} = \phi_a \phi_b \quad (\text{A. } 13)$$

with ϕ_a on atom A and ϕ_b on atom B.

The overlap integrals have the condition that

$$S_{ab} = \begin{cases} 0 & \phi_a \neq \phi_b \\ 1 & \phi_a = \phi_b \end{cases} \quad (\text{A. } 14)$$

This condition for the case in which $\phi_a(1)$ and $\phi_b(1)$ are both on the same center, $A = B$.

APPENDIX A. THE OVERLAP INTEGRALS AND SLATER INTEGRALS

To calculate the overlap integral for two-center case, using the Slater functions of ϕ_a and ϕ_b and transforming these functions to prolate spheroidal coordinates, the overlap integral becomes in final form

$$S_{ab}(n_a, l_a, m, n_b, l_b, \alpha, \beta) = N_a N_b \times \left(\frac{R}{2} \right)^{n_a + n_b + 1} s(n_a, l_a, m, n_b, l_b, \alpha, \beta) \quad (\text{A.15})$$

Where

$$N_a N_b = \frac{(2\zeta_a)^{n_a + \frac{1}{2}} (2\zeta_b)^{n_b + \frac{1}{2}}}{[(2n_a)!(2n_b)!]^{1/2}} \quad (\text{A.16})$$

The overlap integral is programmed in this form, using the subroutine for the reduced overlap integral. On the other hand, the two electron integrals for the s and p orbitals can be calculated by using Slater integrals. The only non vanishing integrals are related to F^0 , G^1 and F^2 mentioned in Eq. (9.9-2.1.1). These integrals have the following forms

$$F^0 = \int_0^\infty \int_0^\infty R_s^*(r_1) R_s^*(r_2) R_s(r_1) R_s(r_2) (2/r_>) r_1^2 r_2^2 dr_1 dr_2 \quad (\text{A.17})$$

$$G^1 = \int_0^\infty \int_0^\infty R_s^*(r_1) R_{px}^*(r_2) R_{px}(r_1) R_s(r_2) (2r_< / r_>) r_1^2 r_2^2 dr_1 dr_2 \quad (\text{A.18})$$

$$F^2 = \int_0^\infty \int_0^\infty R_{px}^*(r_1) R_{py}^*(r_2) R_{px}(r_1) R_{py}(r_2) (2r_<^2 / r_>^3) r_1^2 r_2^2 dr_1 dr_2 \quad (\text{A.19})$$

Where R_s and R_{px} are the radial part of the s and p_x orbitals respectively. $r_<$ and $r_>$ are the smallest and largest values of r_1 and r_2 respectively. (r_1 and r_2 are defined in the equation of the two electron integral).

APPENDIX B. TWO-CENTER AND ONE-CENTER COULOMB
INTEGRALS IN INDO APPROXIMATION

$$\gamma(\mathbf{n}_a, \mathbf{n}_b, \zeta_a, \zeta_b, 0) = \frac{(2\zeta_a)^{2n_a+1}}{(2n_a)!} \left[\frac{(2n_a-1)!}{(2\zeta_a)^{2n_a}} - \sum_{l=1}^{2n_b} \frac{l(2\zeta_b)^{2n_b-l} [2(n_a+n_b)-l-1]!}{(2n_b-l)! 2n_b [2(\zeta_a+\zeta_b)^{2(n_a+n_b)-l}]} \right] \quad (\text{B. } \xi)$$

This integral is also programmed in the present work. The full discussion of the calculation of the two and one center integrals are found in reference [9].

Certification

We certify that this thesis was prepared under our supervision at Babylon University as a partial requirement for the degree of Master of Science in Physics.

Supervisors:

Signature:

Name: *Dr. Mudar A. Abdul-Sattar*

Title: Assist. Prof.

Address: Ministry of Science
and Technology

Date: / / ٢٠٠٥

Signature:

Name: *Dr. Ahmed M. Abdul-Lettif*

Title: Assist. Prof.

Address: University of Babylon

Date: / / ٢٠٠٥

In view of the available recommendations, I forward this thesis for debate by the Examining Committee.

Signature:

Name: *Dr. Talib Hadi Kadouri*

(Head of the Physics Dep.)

Date: / / ٢٠٠٥

Examining Committee Certificate

We certify that we have read this thesis entitled “**Self-Consistent Field Calculations for the Effect of Pressure and Temperature on Some Properties of Grey Tin Crystal**” and, as an Examining Committee, examined the student “**Mohammad Ghanim Merdan** ” in its content and that, in our opinion it meets the standards of a thesis for the degree of Master of Science in Physics.

Signature:
Name: *Dr. Mahdi H. Suhail*
Title: Asist. Prof.
Address: University of Baghdad
Date: / / ٢٠٠٥
(Chairman)

Signature:
Name: *Dr. Fouad S. Hashim*
Title: Asist. Prof.
Address: University of Babylon
Date: / / ٢٠٠٥
(Member)

Signature:
Name: *Dr. Raad M. Saleh Al-Haddad*
Title: Asist. Prof.
Address: University of Baghdad
Date: / / ٢٠٠٥
(Member)

Signature:
Name: *Dr. Mudar A. Abdul-Sattar*
Title: Assist. Prof.
Address: Ministry of Science
and Technology
Date: / / ٢٠٠٥
(Supervisor)

Signature:
Name: *Dr. Ahmed M. Abdul-Lettif*
Title: Assist. Prof.
Address: University of Babylon
Date: / / ٢٠٠٥
(Supervisor)

Approved by the Council of the College of Science.

Signature:
Name: *Dr. Oda Misi'l Yasser Al-Zamehy*
Title: Prof.
Address: University of Babylon
(Dean of the College of Science)
Date: / / ٢٠٠٥

1.1 Preface

Semiconductors are widely used and have important applications in industry and technology specially in instruction of the electronic devices, thus there are many studies of the electronic structure and physical properties of the semiconductors. The semiconductors have different uses according to the difference of their physical properties. The semiconducting grey tin, that is one of the phases of tin, has important uses due to its specific characteristics. So, many workers have studied the energy bands and physical properties of this element, as well as the variation of these properties under the external effects such as pressure. Some of these studies are of theoretical styles based on quantum mechanics. The origin of quantum mechanics is based on the Bohr's (1913) and deBroglie's (1924) assumptions [1]. The first assumption is that electrons move in fixed orbits around the nucleus. This leads to the idea that the angular momentum of electrons in atoms is quantized rather than continuous. DeBroglie has observed that classical mechanics does not describe the behavior of electrons, and he has introduced the principle of wave-particle duality. Schrödinger (1926) has derived the familiar equation (Schrödinger equation) which depends on these assumptions. The Schrödinger equation is generalized for any system, and solving it gives the total energy of the system, and some physical properties can be obtained. On the other hand, the exact solution of Schrödinger equation for a complicated system, which consists of many electrons atoms, is impossible because of a huge number of mathematical processes. For solving such equations, many approximations in the theory are needed, and the use of the computer programming is necessary. The purpose of the large number of approximations in the theory is to maintain the ability of computers for solving such equations [2]. In the

CHAPTER 1. INTRODUCTION

present work, a theoretical model, which is called the large unit cell-intermediate neglected of differential overlap (LUC-INDO) method, is used to calculate some properties of grey tin crystal, and to study the effect of pressure and temperature on these properties.

1.1 *Crystal Binding*

The force that holds crystal together is the attractive electrostatic interaction between the negative charges and the positive charges of solid [1]. Other forces such as gravitational forces and magnetic forces have only a weak effect on cohesion. The energy deficit of a crystal compared with isolated atoms is known as the cohesive energy, and this energy when added to the crystal separates its component into neutral free atoms at rest. The different classes of solid may be associated with different variants of the coulomb attractive forces (bonds) [2,3] and the Van der Waals bonds which arise from the attractive interaction of the induced dipole moments of atoms such as in benzene [4]. The ionic bond is familiar in the case of the NaCl molecule and the coulomb interaction between oppositely charged ions leads to a regular three-dimensional structure. The bond that connects the H₂O molecules in ordinary ice is the hydrogen bond. In this type of bonds, the hydrogen atom can involve itself in an additional electrostatic bond with a second atom of highly electronegative character such as oxygen or to a smaller extent with nitrogen [5]. The metallic bond is familiar in some metals. The interaction of ion cores with the conduction electrons makes a large contribution to the binding energy in metal crystals [6]. The other form of bonding in solid is the covalent bond and will be discussed in the next section.

1.3 Covalent Bond

This is a particularly important bonding mechanism in organic chemistry, and it is also significant in inorganic substances. The C (diamond), Si, Ge and grey tin elements all have four valence electrons and, therefore, a half-filled sp^3 shell. They need four more electrons to form the particularly stable sp^3 octets that characterize the rare gases. The covalent bond is usually formed from two electrons, one from each atom participating in the bond. The electrons forming the bond tend to be partly localized in the region between the two atoms joined by the bond. The spins of the two electrons in the bond are antiparallel [3]. Therefore, each atom associates with four neighboring atoms by the covalent bond as shown in Fig. (1.1) [4].

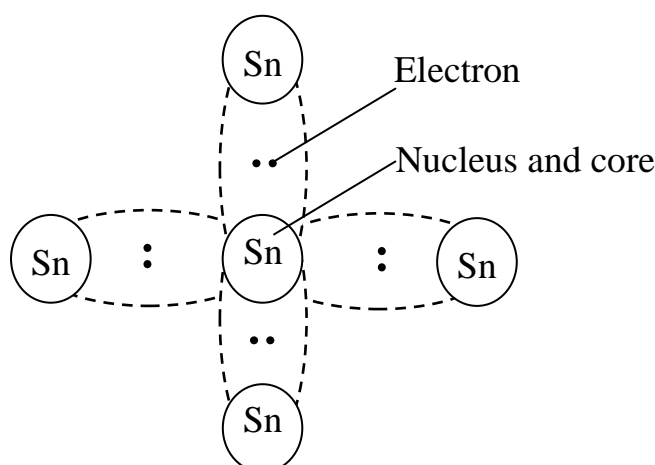


Fig. (1.1) The covalent bond in two dimensions [4]

1.4 Grey Tin Structure

The semiconducting grey tin crystallizes in the same structure of diamond, Si and Ge which is based on the face-centered cubic (fcc) with the basis $\dots, \frac{1}{4} \frac{1}{4} \frac{1}{4}$ as in Fig. (1.2). In this figure the atomic position in the cubic cell of the diamond structure projects on a cube face; fractions denote height above the base in units of a cube edge.

CHAPTER 1. INTRODUCTION

The point at \cdot and $\frac{1}{2}$ are on the (fcc) lattice; those at $\frac{1}{4}$ and $\frac{3}{4}$ are on similar lattice displaced along the body diagonal by one-fourth of its length [3].

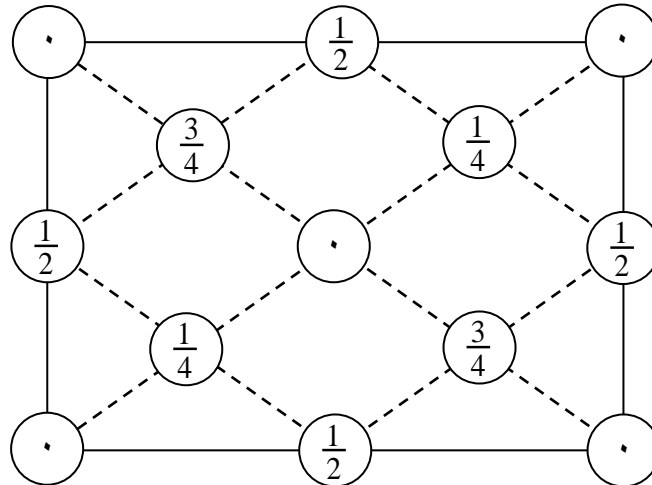


Fig. (1.2) The atomic position in grey tin structure [3]

Thus, the conventional unit cube contains eight atoms and the grey tin crystal is shown in Fig. (1.3). Each atom has ξ nearest neighbors [4, 6].

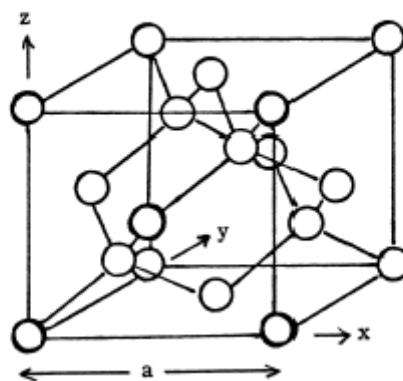


Fig. (1.3) Crystal structure of grey tin [3]

1.2 Hybrid Orbitals of Grey Tin

Tin has the atomic number $Z=50$ and four electrons in the valence band, and has the following configuration,

$$1s^2 2s^2 2p^6 3s^2 3p^6 4s^2 3d^{10} 4p^6 5s^2 4d^{10} 5p^2.$$

We know that in grey tin crystal, each atom makes a covalent bond with four atoms. To provide four unpaired electrons, one of the $5s$ electrons is promoted to the empty $5p$ orbital [^] for giving the following configuration,

$$1s^2 2s^2 \dots \dots \dots 5s^1 5p_x^1 5p_y^1 5p_z^1$$

This configuration would then be expected to form three bonds at right angles to one another and a fourth weak bond with its s orbital in any direction. These four equivalent directed orbitals constitute a set of hybrid orbitals and are commonly referred to as sp^3 hybrids to indicate that they are formed by the combination of one s and three p orbitals.

The general phenomenon of such a combination of pure orbitals is termed hybridization, and the resulting orbitals are called hybrid orbitals. We can write the four valence orbitals of grey tin as $\phi(5s)$, $\phi(5p_x)$, $\phi(5p_y)$ and $\phi(5p_z)$. These are to be combined in suitable proportions to produce new orbitals ψ_1, ψ_2, ψ_3 and ψ_4 as in the following [^].

$$\psi_1 = \frac{1}{2} [\phi(5s) + \phi(5p_x) + \phi(5p_y) + \phi(5p_z)] \quad (1.1)$$

$$\psi_2 = \frac{1}{2} [\phi(5s) + \phi(5p_x) - \phi(5p_y) - \phi(5p_z)] \quad (1.2)$$

$$\psi_3 = \frac{1}{2} [\phi(5s) - \phi(5p_x) + \phi(5p_y) - \phi(5p_z)] \quad (1.3)$$

$$\psi_4 = \frac{1}{2} [\phi(5s) - \phi(5p_x) - \phi(5p_y) + \phi(5p_z)] \quad (1.4)$$

1.7 The Energy Bands and High Symmetry Points

In the case of isolated atoms, the electrons have a definite energy levels. But in the ordinary state these atoms are found together, thus the electron in any orbit will be affected by the neighboring atoms depending on the distances between the electron and nuclei. So, the electrons have energy levels slightly differ between one and another and hence the energy levels of electrons in any orbit form an energy band. The upper energy band is called the valance band. When the valence electron gets a sufficient energy it can rise to the conduction band where it can move freely, leaving behind a hole which behaves like a positive charge carrier equal in magnitude to that of the electron as shown in Fig (1.4). There is a region of forbidden energies between these energy bands. The separation between the conduction and valence band is called the band gap [V].

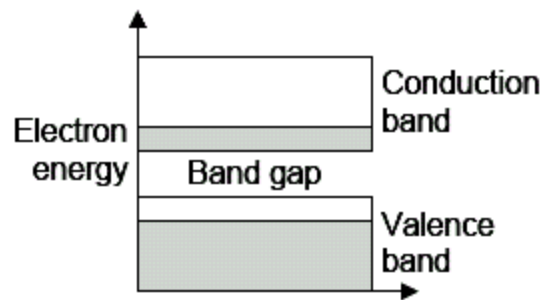


Fig (1.4) Electron behaviour in semiconductors [V].

On the other hand the hybrid orbitals (ψ_1 through ψ_4) have a maximum charge distribution in the direction $[111]$, $[1\bar{1}\bar{1}]$, $[\bar{1}1\bar{1}]$ and $[\bar{1}\bar{1}1]$ respectively. The first neighboring atoms for one atom have their bonds in the direction $[\bar{1}\bar{1}\bar{1}]$, $[11\bar{1}]$, $[1\bar{1}1]$ and $[\bar{1}11]$. The crystal levels will be a linear combination of these new levels on each atom. The crystal orbitals have a definite linear combination in terms of original s and p

CHAPTER 1. INTRODUCTION

orbitals of the free atoms [12]. This linear combination of these atomic orbitals (LCAO) is shown in Table (1.1).

Table (1.1): Some high symmetry Γ points as a (LCAO). s_1 indicates the s orbital on the first atom, s_2 indicates the s orbital on one of the first neighboring atoms [12].

High symmetry points	LCAO
Γ_1	$s_1 + s_2$
Γ_2	$s_1 - s_2$
Γ_{15}	$p_{x1} + p_{x2}$ $p_{y1} + p_{y2}$ $p_{z1} + p_{z2}$
Γ_{25}	$p_{x1} - p_{x2}$ $p_{y1} - p_{y2}$ $p_{z1} - p_{z2}$

The point Γ_1 is the bonding state for the s wavefunctions as in molecular physics, while Γ_{15} is the bonding state for p wavefunctions. The point Γ_2 is the anti-bonding state for the s states, while Γ_{25} is the anti-bonding state for p states [12]. Similar combinations for other high symmetry points that are listed in Table (1.2) are formed at other points of k space. However for each $\Gamma(x, y, z)$ point there is three x point in the directions $(1, y, z)$, $(x, 1, z)$ and $(x, y, 1)$ of the crystal.

Table (1.2): Some high symmetry points in the band structure of solids in units of $(2\pi/a)$ where a is the lattice constant [13].

High symmetry points	Coordinates in k space $(2\pi/a)$
Γ	$(0, 0, 0)$
X	$(1, 0, 0)$
L	$(1/2, 1/2, 1/2)$
K	$(3/4, 3/4, 0)$
Δ	$(1/2, 0, 0)$

W	$(1, 1/2, 0)$
Σ	$(1/2, 1/2, 0)$

The X points that are in the valence band are similar to the Γ_1 and Γ_{25} points, these points are labeled X_{1v} and $X_{\epsilon v}$. The X points that are in the conduction band and are similar to the Γ_2 and Γ_{15} points, are labeled X_{1c} and $X_{\epsilon c}$ [13]. Fig. (1.9) shows the high symmetry points of grey tin listed in Table (1.4). The band structure of $(\alpha - \text{Sn})$ which contains these high symmetry points can be shown from Akdim *et al.* work [13]. They used the linearized augmented plane-wave (LAPW) calculations and tight-binding (TB) method.

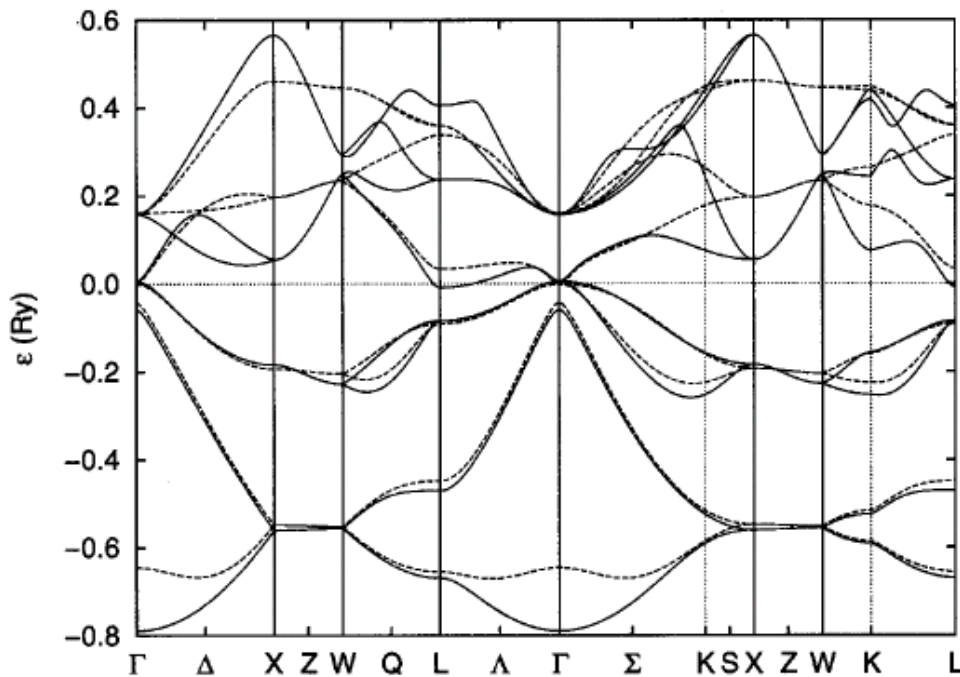


Fig.(1.9) Band structure of grey tin at the experimental lattice constant, (—),first principles LAPW calculations; (----), TB results. In both calculations they set the Fermi level to zero. The energies are in rydberg (1 Ry is the binding energy of an electron in a hydrogen atom and is equal to 13.606 eV) [13].

1.4 Tin Phases

Tin has two allotropic forms, white (β) or ordinary tin, and grey (α) tin, which have been discussed in the previous sections. The β -Sn phase is a tetragonal with two atoms per unit cell [16] as shown in Fig. (1.6) [17]. Grey tin is greyish powder with lower density than white tin and is formed by cooling of high purity white tin at temperature below $(13.2)^{\circ}\text{C}$ [18-20]. Some properties of tin are listed in Table (1.3).

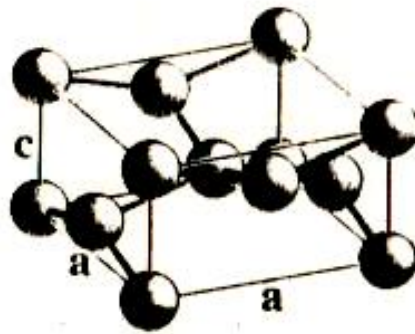


Fig (1.6) The β -Sn structure with lattice constants a and c [17].

Table (1.3): Some properties of tin [18]

Property	Value	
Atomic no	50	
Valence	4	
Melting point	231.9°C	
Boiling point	260.2°C	
Density	5.77^a	(g/cm^3)
	7.27^b	

^a Grey tin

^b White tin

1.1 Phase Transitions in Tin

The ($\alpha \leftrightarrow \beta$) transition can be experimentally observed when the temperature is raised above 13.2°C or ($\sim 286\text{K}$) [11]. Also, this transition occurs at 1 GPa [16]. On application of pressure to the β phase, an abrupt transition to a body-centered-tetragonal (bct) phase is observed experimentally at about 9.0 GPa, and from this to a body-centered-cubic (bcc) phase at pressure between 4.0 and 6.0 GPa [11]. Thus the sequence of transitions is $\alpha\text{-Sn} \rightarrow \beta\text{-Sn} \rightarrow \text{bct} \rightarrow \text{bcc}$.

There are other phases of tin can be shown in the phase diagram of tin (Fig. (1.1)) [16].

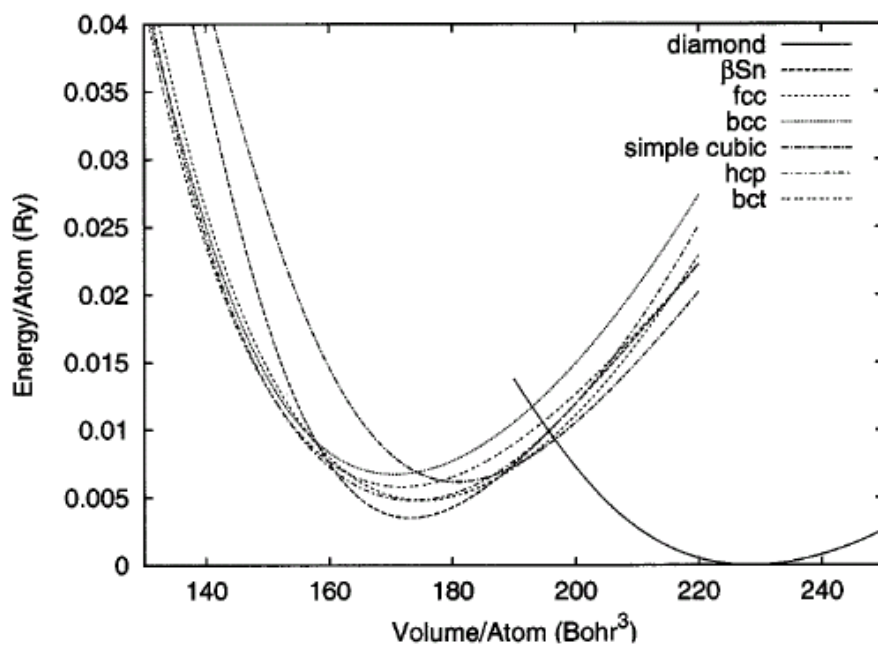


Fig (1.1) Tin phase diagram [16].

1.4 Literature Survey

1. In 1963, Bassani and Liu [22], studied the electronic band structure including spin-orbit coupling for semiconducting grey tin. They used the plane-wave method to obtain the energy eigenvalues at the symmetry points Γ , X and L in the Brillouin zone and to compute the spin-orbit splittings at these points. They found that both the conduction band and valence band edges were at the center of the zone. They calculated the effective masses for electrons and holes and the effect of pressure on energy band. The properties which were calculated had good agreement with experimental results.
2. In 1970, Pollak *et al.* [23], used the first principles of relativistic orthogonalized-plane-wave calculation to determine the energy eigenvalues of grey tin at seven key point of the reduced zone. Optical constants and derivative optical constants were calculated from $\tilde{\kappa}, \tilde{p}$ parameters. Valence band mass parameters, effective masses, and g factors at several points in the zone were calculated and their values were in good agreement with experimental values.
3. In 1971, Buchenauer *et al.* [24], studied the first order one-phonon Raman spectrum of grey tin and its temperature dependence. Their calculations included the bulk modulus and the calculated value was in good agreement with that determined by experiments.
4. In 1979, Harker and Larkins [25], calculated some properties of diamond and silicon crystals using a large unit cell-complete neglect of differential overlap (LUC-CNDO) crystal orbital approach. They calculated lattice constant, cohesive energy, bulk modulus, hybridization states and energy band. Some of these properties were in good agreement with experimental values.

CHAPTER 1. INTRODUCTION

- . In 1987, Svane [14], used Hartree-Fock approximations based on the linear muffin-tin-orbital (LMTO) method for calculating electronic structure of diamond, Si, Ge and α -Sn. The frozen core approximation was used and relativistic effects were incorporated through the scalar relativistic approximation. The calculations of cohesive energy and electronic structure were in agreement with the previous Hartree-Fock and experimental calculations.
- ¶. In 1988, Van Camp *et al.* [16], calculated some ground-state and electronic properties of the covalent semiconductors (C, Si, Ge and α -Sn). They derived these properties from the total crystalline energy. The calculated properties were the lattice constant, bulk modulus, pressure coefficients of the bulk modulus, and the energy difference between the top valence band and the lowest conduction band. The calculated values were in agreement with experimental values.
- ∇. In 1997, Abdul-Sattar [13], used a large unit cell-intermediate neglect of differential overlap (INDO) crystal orbital approach (LUC-INDO) rather than (LUC-CNDO) to calculate some physical properties of covalent elements (C, Si, Ge and α -Sn). He added the correlation corrections to the previous calculations made by other investigators to simulate the crystal band structure and physical properties of the aforementioned semiconductors. Most of the properties which were calculated by this model were in good agreement with experimental values.
- ∧. In 1998, Pavone *et al.* [15], studied the $\alpha \leftrightarrow \beta$ transition in tin. The free energies of α and β phases of tin were calculated in harmonic approximation using density functional theory and density functional perturbation theory, within the local density

CHAPTER 1. INTRODUCTION

approximation. They found that the narrower the frequency range spanned by the vibrational band in the β phase was, the larger its entropy was made at high temperature. As a consequence, the free energies of the phases equal each other at a temperature of 38°C , and this was in close agreement with the transition temperature 37.2°C .

9. In 1999, Xie *et al.* [28], studied the thermodynamic properties of diamond at high pressure (up to 1000 GPa) by using ab-initio pseudopotential plane wave method and the density-functional perturbation theory. They studied the effect of pressure and temperature on lattice constant and bulk modulus. They found that the thermal expansion coefficient decreases with the increase of pressure, the phonon frequency at X_4 and L'_3 gradually goes higher than that of X_1 and L'_2 respectively and the unusual overbending of the upper most phonon dispersion curves near Γ'_{25} decreases with the increase of pressure.
10. In 2001, Pavone [29], reported an overview of the basic lattice dynamics. Starting from the classical formulation, a tutorial description of the evaluation of the lattice dynamical was reported, paying special attention to the method based on the density functional theory. Among these methods was the perturbative ab initio approach. He gave some applications of this formalism to some cases of general interest. In particular he reported on controversy about the origin of a peak in the second order Raman spectrum of diamond and on the temperature-induced phase transitions in tin.

CHAPTER 1. INTRODUCTION

11. In 2001, Asokamani and Rita [30], studied the band structure of ABC_3 (A=Zn, B=Si, Ge, Sn and C=P, As) ternary pnictides performed using the semi-relativistic "tight binding linear muffin tin orbital" (TB-LMTO) method within local density approximation. Energy gap at ambient pressure was found to be direct in all the cases. They calculated the equilibrium lattice constant, the bulk modulus from the total energy calculation. More generalized equating cell volume V_c and microhardness (H) as well as V_0 and melting point θ_m for pnictides were established. The values of H and θ_m for some pnictides were predicted for the first time in cases where experimental values were not known.
12. In 2002, Akdim *et al.* [16], used the Naval Research Laboratory (NRL) tight-binding (TB) method to study the bulk properties of both α -Sn and β -Sn. The parameters were determined by fitting data base of first-principles band structure and total energies, using the general potential linearized augmented plane-wave method for the fcc, bcc, sc and diamond structures, with limited information from calculations of the β -Sn phase. They discussed the NRL-TB method's ability to calculate electronic band structures and density of states. They calculated the elastic constants of α -Sn and β -Sn as well as several high-symmetry point phonon frequencies of α -Sn, and TB molecular dynamics calculations were used to explore the behaviour of tin at finite temperatures.
13. In 2003, Mujica *et al.*[21], advanced the accuracy and efficiency of first-principles electronic structure calculations which allowed detailed studies of the energetics of materials under high pressures. At the same time, improvements in the resolution of

CHAPTER 1. INTRODUCTION

power X-ray diffraction experiment and more sophisticated methods of data analysis have revealed the existence of many new unexpected high-pressure phases of tin. The most complete set of theoretical and experimental data obtained to date was for the group IVA element and group IIIA-VA and IIB-VIA compounds. Their studies included the phase transition in tin.

14. In 2003, Olguin *et al.* [31], introduced a theoretical study for the effect of hydrostatic pressure on interatomic bond lengths and energy band gaps of γ -InSe. Total energy calculations were performed using the linear augmented plane wave (LAPW) method, taking into account scalar relativistic corrections as well as spin-orbit coupling. They found that the covalent In-In bonds were oriented to be more compressible than the partially ionic In-Se bond. They also calculated pressure dependence of band gap. Most of their calculations were in good agreement with the experimental results.

1.1 • *The Research Objective*

Tin has many applications. For example, it is used to form many useful alloys. Bronze is an alloy of tin and copper. Tin and lead are alloyed to make pewter and solder. On the other hand tin becomes a superconductor below 3.72 K. In fact, tin was one of the first superconductors to be studied. The Meissner effect which is one of the characteristic features of superconductors, was first discovered in superconducting tin crystals. The niobium-tin compound Nb₃Sn is commercially used as wires for superconducting magnets. Because of these important applications of tin, especially grey tin, the study of its electronic structure and other physical properties is necessary.

CHAPTER 1. INTRODUCTION

The aim of the present work is to apply the self-consistent field calculations represented by the large unit cell within intermediate neglect of differential overlap (LUC-INDO) method to study the electronic structure and some physical properties of grey tin crystal. Correlation correction and relativistic effects can be taken into account to obtain precise results. This method may be used to investigate the variation of properties with pressure and with temperature. Thus, we think that calculation of the external effects such as pressure and temperature is necessary in industry and applications.

The (LUC-INDO) method has been chosen in the present work rather than other methods because this method can be used to give reliable and precise results with relatively short time. This method is used to study the properties of grey tin in the present work below 1 GPa and temperature range below 13.2 °C because beyond these limits tin has phase transition to (β -Sn).

2.1 The Schrödinger Equation

Based on deBroglie's wave-like description of electrons, Schrödinger combined the quantum assumptions of Bohr with the wave equations of classical mechanics to yield a new description of electrons. In mechanics, the total energy of a system of particles can be described in terms of particle momenta and coordinates. For time-independent systems in classical motion [५५-५६]

$$E = KE \text{ (kinetic energy)} + PE \text{ (potential energy)} \quad (५.१)$$

The kinetic energy of an electron is given by:

$$KE = (1/2)mv^2 = \frac{p^2}{2m} \quad (५.२)$$

Where m is the mass of electron, v is the electron's velocity, and p is the electron's momentum.

The potential energy for an electron moving in the field of a nucleus of charge Ze ,

$$PE = -Ze^2r^{-1} \quad (५.३)$$

where r is the distance of the electron from the nucleus and e is the unit of electronic charge.

Thus the total energy of the electron is the sum of a kinetic energy contribution and potential energy function,

$$E = \frac{p^2}{2m} - Ze^2r^{-1} \quad (५.४)$$

CHAPTER १. THEORY

The equation can be converted to a form suitable for use in quantum mechanics,

$$\left\{ -\frac{\hbar^2}{2m} \nabla^2 - \frac{Ze^2}{r} \right\} \psi(1) = E\psi(1) \quad (१.९)$$

where

\hbar : Plank constant (h) divided by 2π

Ψ : a wavefunction of the electron

∇^2 : Laplacian operator (kinetic energy operator)

$$\nabla^2 = \frac{\partial^2}{\partial x^2} + \frac{\partial^2}{\partial y^2} + \frac{\partial^2}{\partial z^2}$$

The operator from the left-hand side of Eq. (१.९) has a special name; it is called the Hamiltonian operator which is symbolized by H . In condensed form, the Schrödinger equation is written as,

$$H\psi(1) = E\psi(1) \quad (2.6)$$

Hamiltonian operator of many electron atoms can be formulated in similar manner. It is again the sum of the kinetic energy operators for the nuclei and for the electrons together with the potential energy terms representing the various coulombic interaction [१९].

$$H^T = T_N + T_e + V_{ee} + V_{eN} + V_{NN} \quad (१.१)$$

Where T_N and T_e are the kinetic energy operators for the nuclei and electrons respectively. V_{ee} , V_{eN} and V_{NN} the potential energy between electron-electron, electron-nucleus and nucleus-nucleus respectively. Suppose that there are N nuclei with n electrons, the total Hamiltonian operator will be,

CHAPTER 2. THEORY

$$H^T = -\frac{1}{2} \sum_A^N \frac{1}{M_A} \nabla_A^2 - \frac{1}{2} \sum_p^{2n} \nabla_p^2 + \sum_{p < d}^{2n} r_{pd}^{-1} - \sum_A^N \sum_p^{2n} Z_A r_{Ap}^{-1} + \sum_{A < B}^N Z_A Z_B R_{AB}^{-1} \quad (2.1)$$

where we have used atomic units: $\hbar = m_e = e = 1$. M_A is the mass of nucleus; m electronic mass; Z_A, Z_B is the charge on nucleus A, B respectively, r_{pd} is the distance between particles p and d and R_{AB} is the distance between nuclei A and B [2, 3]. The general form of Schrödinger equation will be,

$$H^T(\mathbf{r}, \mathbf{r}, \dots, N, \mathbf{r}, \mathbf{r}, \dots, n) \Psi(\mathbf{r}, \mathbf{r}, \dots, N, \mathbf{r}, \mathbf{r}, \dots, n) = E \Psi(\mathbf{r}, \mathbf{r}, \dots, N, \mathbf{r}, \mathbf{r}, \dots, n) \quad (2.2)$$

where Ψ is the complete wavefunction for all particles in the molecule and E is the total energy of the system.

2.2 The Born-Oppenheimer Approximation

Representation of the complete wavefunction as a product of an electronic and a nuclear part gives:

$$\Psi(r, R) = \Psi_e(r, R) \Psi_N(R) \quad (2.3)$$

Here r is used to denote the positions and the spins of the electrons, i.e. $(r_1, s_1, r_2, s_2, \dots)$. R denotes the nuclear coordinates (R_1, R_2, \dots) .

where the two wavefunctions may be determined separately by solving two different Schrödinger equations [3-5]. On the other hand, the nuclei are much heavier than the electrons and the mass of the nuclei are several thousand times larger than the masses of the electrons, so that the nuclei move much more slowly, the Born Oppenheimer approximation separates the nuclear kinetic energy and nuclear-nuclear repulsion terms from H^T , and considers only the part of the Hamiltonian which depends on the position but not the momenta of nuclei [6-8]. the electronic Hamiltonian operator is given as,

CHAPTER 2. THEORY

$$H^{el} = -\frac{1}{2} \sum_p^{2n} \nabla_p^2 - \sum_A^N \sum_p^{2n} \frac{Z_A}{r_{Ap}} + \sum_{p<d}^{2n} \frac{1}{r_{pd}} \quad (2.11)$$

We can use electronic Hamiltonian to modify Schrödinger equation as,

$$H^{el}(\psi, r, \dots, n) \Psi(\psi, r, \dots, n) = \varepsilon \Psi(\psi, r, \dots, n) \quad (2.12)$$

The solution of the above equation describes the motion of the electrons in the field of the fixed nuclei. The total energy E of a given internuclear distance is then given by

$$E = \varepsilon + \sum_{A<B} Z_A Z_B R_{AB}^{-1} \quad (2.13)$$

Where ε is the electronic energy and the second term is the electrostatic internuclear repulsion energy [2, 13].

2.2 The Variational Method

The complete treatment of quantum mechanical problem involving electronic structure is equivalent to the complete solution of the appropriate Schrödinger equation. A direct approach in terms of mathematical treatment of the partial differential equation is practicable only for one electron system, but for many electron atoms the solution can be obtained by variational method [2, 14]. This method is equivalent to differential equations, The variational principle states that the energy computed from the expectation value of the Hamiltonian operator will always be larger than or equal to the true ground state energy for the system [2, 14, 15].

$$\frac{\int \Psi^* \hat{H} \Psi d\tau}{\int \Psi^* \Psi d\tau} = E_{\text{var}} \geq E_{\text{exact}} \quad (2.14)$$

CHAPTER 2. THEORY

In quantum mechanics we deal with approximate wavefunction for a molecular system which when substituted into the Schrödinger equation, will always yield higher energy than the actual energy of the system. When Ψ is a complete wavefunction, the solution of Schrödinger equation gives stationary values of the energy. Therefore, a small change $\delta\Psi$

$$\delta\varepsilon = \delta \langle \Psi | H | \Psi \rangle = \dots \quad (2.15)$$

The advantage of this method is that the same criteria can be applied to incomplete wavefunctions to obtain approximations to correct wavefunctions. So we can apply this method when Ψ is a function of numerical parameters c_1, c_2, \dots as linear combination of fixed function Φ_1, Φ_2, \dots

$$\Psi(c_1, c_2, \dots) = c_1 \Phi_1 + c_2 \Phi_2 + \dots \quad (2.16)$$

And the stationary values of ε will satisfy

$$\delta\varepsilon = \frac{\partial\varepsilon}{\partial c_1} \delta c_1 + \frac{\partial\varepsilon}{\partial c_2} \delta c_2 + \dots = 0 \quad (2.17)$$

2.4 The Hartree Approximation

Another common approximation is to construct a specific form for the many body wavefunction. If one can obtain an accurate wavefunction, then via the variational principle an accurate estimate for the energy will emerge. The most difficult part of this exercise is to use physical intuition to define a trial wavefunction close to the true wavefunction. The total wavefunction for n electron system is generally approximated as a product of the one electron functions $\psi_1, \psi_2, \dots, \psi_n$

CHAPTER 2. THEORY

$$\Psi(r_1, r_2, \dots, r_n) = \psi_1(r_1) \psi_2(r_2) \psi_3(r_3) \dots \psi_n(r_n) \quad (2.18)$$

Such one electron functions ψ_n are called orbitals, and the product function as such is known as a Hartree product [26, 27]. Therefore, the many electron Hamiltonian $H^{el}(r_1, r_2, \dots, r_n)$ could be written as a sum of one electron operators $\mathcal{H}(P)$

$$H^{el}(r_1, r_2, \dots, r_n) = \sum_P \mathcal{H}(P) = \sum_P \left[-1/2\nabla_P^2 + V(P) \right] \quad (2.19)$$

where $V(p)$ is an unspecified one electron potential energy function.

This form of Hamiltonian is used in Schrödinger equation of the system

$$H^{el}(r_1, r_2, \dots, r_n) \Psi(r_1, r_2, \dots, r_n) = \varepsilon \Psi(r_1, r_2, \dots, r_n) \quad (2.20)$$

The Hamiltonian for p th electron is

$$\mathcal{H}(P) = -1/2\nabla_P^2 + V(P) \quad (2.21)$$

We can write one electron Schrödinger equation of individual orbitals ψ_i as the form

$$\mathcal{H}(r_i) \psi_i(r_i) = \varepsilon_i \psi_i(r_i) \quad (2.22)$$

Where ε_i is the orbital energy.

2.5 The Hartree-Fock Approximation

Until now we have not taken into account the spin of the electrons. According to Pauli exclusion principle: a maximum of two electrons can occupy an orbital and the spin of the electrons are paired (i.e opposed). The z component of the spin angular momentum is quantized and has two

CHAPTER 7. THEORY

possible values $\mp \frac{1}{2}$ in the unit of $\frac{h}{2\pi}$. These two spin states may be represented by two mutually orthogonal spin wavefunctions; α which belongs to $+\frac{1}{2}$ state and β which belongs to $-\frac{1}{2}$ state [2.21]. Therefore, the complete wavefunction for a single electron is a product of spatial function and spin function,

$$\Psi(\mathbf{r}) = \psi(\mathbf{r}) \eta(\mathbf{r}) \quad (2.22)$$

Where $\eta(\mathbf{r})$ may be associated with either α or β spin function.

On the other hand, electrons are Fermions. The minimum requirements for a many-fermion wavefunction are antisymmetry with respect to interchange of electrons and indistinguishability of the electrons [2.22-2.23]. Thus, no physical property of the system can change if we simply rename or renumber the electrons. Mathematically, Ψ must be antisymmetric with respect to an exchange of the coordinates of two electrons for example by the permutation operator $P_{1,2}$:

$$P_{1,2}\Psi(\mathbf{r}_1, \mathbf{r}_2) = -\Psi(\mathbf{r}_1, \mathbf{r}_2) \quad (2.24)$$

The total wavefunction of two electron as a Hartree product does not satisfy antisymmetric principle. Consider

$$\Psi(\mathbf{r}_1, \mathbf{r}_2) = \psi_1(\mathbf{r}_1)\alpha(\mathbf{r}_1)\psi_2(\mathbf{r}_2)\beta(\mathbf{r}_2) - \psi_1(\mathbf{r}_2)\alpha(\mathbf{r}_2)\psi_2(\mathbf{r}_1)\beta(\mathbf{r}_1) \quad (2.25)$$

Now

$$P_{1,2}\Psi(\mathbf{r}_1, \mathbf{r}_2) = \psi_1(\mathbf{r}_2)\alpha(\mathbf{r}_2)\psi_2(\mathbf{r}_1)\beta(\mathbf{r}_1) - \psi_1(\mathbf{r}_1)\alpha(\mathbf{r}_1)\psi_2(\mathbf{r}_2)\beta(\mathbf{r}_2) \quad (2.26)$$

The result of $P_{1,2}\Psi(\mathbf{r}_1, \mathbf{r}_2)$ is seen to be $-\Psi(\mathbf{r}_1, \mathbf{r}_2)$ as desired. Therefore, $\Psi(\mathbf{r}_1, \mathbf{r}_2)$ is an acceptable wavefunction. Notice that $\Psi(\mathbf{r}_1, \mathbf{r}_2)$ is the determinant of a simple matrix

CHAPTER 7. THEORY

$$\Psi(\mathbf{r}, \tau) = \frac{1}{\sqrt{2}} \begin{vmatrix} \psi_1(1)\alpha(1) & \psi_1(1)\beta(1) \\ \psi_1(2)\alpha(2) & \psi_1(2)\beta(2) \end{vmatrix} \quad (7.27)$$

Generalizing the previous equation to give n electrons system determinant can be as follow [7, 28, 29]:

$$\Psi(\mathbf{r}, \tau, \dots, n) = \frac{1}{\sqrt{2n!}} \begin{vmatrix} \psi_1(1)\alpha(1) & \psi_1(1)\beta(1) & \psi_2(1)\alpha(1) & \dots & \psi_n(1)\beta(1) \\ \psi_1(2)\alpha(2) & \psi_1(2)\beta(2) & \dots & \dots & \psi_n(2)\beta(2) \\ \dots & \dots & \dots & \dots & \dots \\ \psi_1(2n)\alpha(2n) & \psi_1(2n)\beta(2n) & \dots & \dots & \psi_n(2n)\beta(2n) \end{vmatrix} \quad (7.28)$$

This form of wavefunction is called Slater determinant [7, 28, 29]. It reflects the proper symmetry of the wavefunction and Pauli principle. Eq. (7.28) can be written as the product of the diagonal elements of the matrix enclosed in bars

$$\Psi(\mathbf{r}, \tau, \dots, n) = |\psi_1(1)\alpha(1)\psi_1(2)\beta(2)\dots\psi_n(2n)\beta(2n)| \quad (7.29)$$

For the one electron wavefunction, the orthonormality condition is applied in the calculation,

$$\int \psi_i \psi_j d\tau = \delta_{ij} \quad (7.30)$$

In this expression, $d\tau$ is the volume element, δ_{ij} denotes the kronecker delta, which is 1 when $i=j$ and 0 otherwise. We notice the factor $\frac{1}{\sqrt{2n!}}$ in the right hand side of Eq. (7.28). This is so because the combination of Hartree products is normalized to unity.

7.7 The Energy Expression for a Closed Shell System

Let's assume a wavefunction of Slater determinate form, and find an expression for the expectation value of the electronic energy for n electrons system,

CHAPTER १. THEORY

$$\varepsilon = \langle \Psi | H_e | \Psi \rangle / \langle \Psi | \Psi \rangle \quad (१.३१)$$

where H_e is the electronic Hamiltonian operator, it may be separated into one and two-electron parts [११, ११]

$$H_e = H_1 + H_2 \quad (१.३२)$$

or

$$H_e = \sum_p H^{\text{core}}(p) + \sum_{p < d} r_{pd}^{-1} \quad (१.३३)$$

where

$$H^{\text{core}}(p) = -\frac{1}{2} \nabla_p^2 - \sum_A Z_A r_{pA}^{-1} \quad (१.३४)$$

Here H^{core} is the one electron Hamiltonian corresponding to the motion of an electron in the field of bare nuclei. The energy expectation value is the sum of the expectation values of the one electron and two electron part [१],

$$\langle \Psi | H_e | \Psi \rangle = \langle \Psi | H_1 | \Psi \rangle + \langle \Psi | H_2 | \Psi \rangle \quad (१.३५)$$

The one electron part is given as,

$$\langle \Psi | H_1 | \Psi \rangle = \sum_p^{2n} \langle \Psi | H^{\text{core}}(p) | \Psi \rangle \quad (१.३६)$$

Eq. (१.३६) is simplified as follows

$$\langle \Psi | H_1 | \Psi \rangle = 2 \sum_{i=1}^n H_{ii} \quad (१.३७)$$

CHAPTER 7. THEORY

where H_{ii} is the expectation value of the one electron core Hamiltonian corresponding to the molecular orbital,

$$H_{ii} = \int \psi_i^*(1) H^{\text{core}} \psi_i(1) d\tau_1 \quad (7.38)$$

The second part of Eq. (7.35) is given as,

$$\langle \Psi | H_2 | \Psi \rangle = \frac{1}{2} (2n)(2n-1) \langle \Psi | r_{12}^{-1} | \Psi \rangle \quad (7.39)$$

where $\left[\frac{1}{2} (2n)(2n-1) \right]$ is the electron-electron repulsion terms and because of the indistinguishability of electrons, each will give the same contribution. The final result of Eq. (7.39) is given as,

$$\langle \Psi | H_2 | \Psi \rangle = \sum_i^n \sum_j^n (2J_{ij} - K_{ij}) \quad (7.40)$$

where J_{ij} is called the coulomb integrals,

$$J_{ij} = \iint \psi_i^*(1) \psi_j^*(2) \frac{1}{r_{12}} \psi_i(1) \psi_j(2) d\tau_1 d\tau_2 \quad (7.41)$$

and K_{ij} is the exchange integral

$$K_{ij} = \iint \psi_i^*(1) \psi_j^*(2) \frac{1}{r_{12}} \psi_j(1) \psi_i(2) d\tau_1 d\tau_2 \quad (7.42)$$

Therefore, the total electronic energy will be,

$$\varepsilon = 2 \sum_i^n H_{ii} + \sum_i^n \sum_j^n (2J_{ij} - K_{ij}) \quad (7.43)$$

This formula contains a set of three and six-dimensional integrals H_{ii} , J_{ij} and K_{ij} [7, 8]. The one electron integral H_{ii} represents the energy of an electron in a molecular orbital ψ_i in the field of bare nuclei, and because

CHAPTER 7. THEORY

there are two electrons in each orbital, this term should be multiplied by 2. The interaction of the smoothed-out charged distribution $\psi_i^*\psi_i$ and $\psi_j^*\psi_j$ is represented by the two electron integral J_{ij} . The second term in Eq. (7.43) comes from the fact that if electrons 1 and 2 are assigned to different spatial molecular orbital ψ_i and ψ_j , both have α or β spin and there will be four contributions each of which equals to $1/2 J_{ij}$. The exchange integral enters with a negative sign and reduces the energy between the electrons with parallel spin in different orbitals ψ_i and ψ_j . Therefore, if the electrons 1, 2 are assigned to different spatial orbital ψ_i and ψ_j , there will be two contribution each of which equals to $1/2 K_{ij}$.

7.4 Hartree-Fock Equations

After getting the proper form for the many electron wavefunction for closed shell system as a single determinant of spin orbitals, and developing a convenient expression for the electronic energy, the variational principle to this expression will be applied. According to this principle, if one adjusts an approximate of many electron wavefunctions as Slater determinate to lower the energy, then the solution of this wavefunction will be approached. one can obtain the best molecular orbitals by varying all the contributing electron functions $\psi_1, \psi_2, \dots, \psi_n$ in Slater determinate to achieve the minimum value of the energy $[\epsilon, \delta\epsilon]$. The variation of ϵ , $(\delta\epsilon)$ is zero to first order,

$$\delta\epsilon = 0$$

The variation of ϵ is written as,

$$\delta\epsilon = 2 \sum_i^n \delta H_{ii} + \sum_i^n \sum_j^n (2\delta J_{ij} - \delta K_{ij}) \quad (7.44)$$

CHAPTER 7. THEORY

Because the variations of the orbitals are linearly independent, one can derive a related equation for a single electron (λ) in a single orbital (i)

$$\left\{ H^{\text{core}}(1) + \sum_j^n [2J_j(1) - K_j(1)] \right\} \psi_i(1) = \varepsilon_i \psi_i(1) \quad (7.45)$$

where

ε_i is the electronic energy of the electron in orbital i .

J_j is the coulomb operator which is defined by

$$J_j(1) = \int \psi_j^*(2) \frac{1}{r_{12}} \psi_j(2) d\tau_2 \quad (7.46)$$

It is the averaged electrostatic potential of the two electrons in the orbital ψ_j .

K_j is the exchange operator and can not be written as a simple function but has the property that

$$K_j(1)\psi_i(1) = \left[\int \psi_j^*(2) \frac{1}{r_{12}} \psi_i(2) d\tau_2 \right] \psi_j(1) \quad (7.47)$$

It is more complicated, and it arises from the effect of the antisymmetry of the total wavefunction on the correlation between electrons of parallel spin. The quantity in large curly brackets in Eq. (7.47) is called the Fock operator $F(\lambda)$. Thus,

$$F(1)\psi_i(1) = \varepsilon_i \psi_i(1) \quad (7.48)$$

These are commonly known as the Hartree-Fock equations which state that the best molecular orbitals are all eigenfunctions of the Fock operator [40, 49, 51].

2.1 Self-Consistent Field Theory (SCF)

This theory is used to calculate the proper wavefunction of the system. It is commonly used to solve the integrodifferential equations after transforming these equations to differential equations [2]. Therefore, in order to evaluate J_j and K_j terms in Eq. (2.10) for the calculation of ψ_i , one needs to know ψ_i . First, assuming a set of trial solution ψ'_1, ψ'_2, \dots allows the computation of coulomb and exchange operators in order to calculate a new eigenfunctions $\psi''_1, \psi''_2, \dots$ of these operators which are the second set of trial functions. This procedure is continued until there is no change in the orbital between iterations [3, 4]. The orbitals are then said to be self-consistent with the field generated by the electrons. Hence, we call this process a Self-Consistent Field (SCF) calculation [5].

2.2 Linear Combination of Atomic Orbitals (LCAO)

For molecular system of any size, direct solution of Hartree-Fock equation is impractical and more approximate methods are required to solve these equations. Therefore, the individual molecular orbitals is required to be expressed as linear combinations of a finite set of N_o prescribed one electron functions known as basis functions. If the basis functions are $\phi_1, \phi_2, \dots, \phi_n$, then an individual orbital ψ_i can be written [6, 7, 8]

$$\psi_i = \sum_{\mu=1}^{N_o} C_{\mu i} \phi_{\mu} \quad (2.19)$$

where $C_{\mu i}$ are the molecular orbital expansion coefficients.

This method has a further advantage that it aids the interpretability of the result, since the nature of chemical problem frequently involves

CHAPTER 2. THEORY

relating properties of molecules to those of the constituent atoms. The orthonormality condition in the LCAO approximation is given as,

$$\sum_{\mu\nu} C_{\mu i}^* C_{\nu j} S_{\mu\nu} = \delta_{ij} \quad (2.50)$$

where δ_{ij} is the kronecker delta and $S_{\mu\nu}$ is the overlap integral for atomic function ϕ_{μ} and ϕ_{ν} ,

$$S_{\mu\nu} = \int \phi_{\mu}(1)\phi_{\nu}(1)d\tau_1 \quad (2.51)$$

2.1 • Basis Sets

The atomic orbitals used for the LCAO procedure form the basis set of the calculation. Selection of the correct basis set is an important decision because it dictates the accuracy and computational difficulty of the calculation. We distinguish here three types of basis sets commonly encountered [2]:

- (1) Valence: only valence orbitals (e.g., 2s and 2p on C).
- (2) Minimal: all orbitals up to and including valence (1s, 2s, and 2p on C).
- (3) Extended: extra functions added to the minimal set (e.g., d on C).

In the atomic problem, we are faced with a spherical symmetry problem. So, the functions contain a radial and an angular function, the latter being simply the spherical harmonics $Y_{lm}(\theta, \phi)$ [22, 23, 24].

We shall thus write an atomic orbital as

$$\phi(\mathbf{r}, \theta, \phi) = R_{nl}(r)Y(\theta, \phi) \quad (2.52)$$

The angular part is defined as

CHAPTER ۲. THEORY

$$Y_{lm}(\theta, \phi) = \theta_{lm}(\theta)\Phi_m(\phi) \quad (۲.۵۳)$$

where, in real space

$$\theta_{lm}(\theta) = \left(\frac{(2l+1)(l-m)!}{2(l+m)!} \right)^{1/2} P_l^m(\cos\theta) \quad (۲.۵۴)$$

$$\Phi_m(\phi) = \begin{cases} (\pi)^{-1/2} \cos m\phi & m \neq 0 \\ (2\pi)^{-1/2} & m = 0 \end{cases} \quad (۲.۵۵)$$

The quantities $P_l^m(\cos\theta)$ are the normalized associated Legendre polynomials, taken in the form [۲]

$$P_l^m(\cos\theta) = \frac{(m+1)!}{8} \sin^m \theta \sum_{u=0}^{l-m} C_{lm u} \cos^u \theta \quad (۲.۵۶)$$

where l , and m are the azimuthal and magnetic quantum numbers respectively, and the coefficients $C_{lm u}$ are determined from the usual form of the associated Legendre polynomials $P_l^m(\cos\theta)$. The different types of orbitals will differ by the form of the radial function R_{nl} . The atomic orbitals also present some peculiarities at the nucleus (i.e. a cusp), and the basis functions should be tried to satisfy those conditions as possible.

There are two types of the function representation of minimal basis sets of the atomic orbitals [۴۵, ۵۳, ۵۵, ۵۶]:

CHAPTER 2. THEORY

2.1.1 Slater-Type Orbitals (STO)

These orbitals have the radial form

$$R_n(r) = N_n r^{n-1} \exp(-\zeta r) \quad (2.57)$$

Where N_n is the radial normalization constant,

$$N_n = \frac{(2\zeta)^{n+1/2}}{[(2n)!]^{1/2}} \quad (2.58)$$

ζ is the orbital exponent, these functions arise from a potential

$$V(r) = -\frac{\zeta n}{r} + \frac{n(n-1) - l(l+1)}{2r^2} \quad (2.59)$$

The Slater-type orbitals constitute good atomic orbital basis for atomic and molecular calculations, but for molecules the evaluation of integral over polycentric functions is quite difficult. The STO is used in this work.

2.1.2 Gaussian-Type Orbitals (GTO)

These very common functions have a radial form

$$R_n(r, \alpha) = N_\alpha r^{n-1} \exp(-\alpha r^2) \quad (2.60)$$

with:

$$N_\alpha = 2^{n+1} [(2n-1)!!]^{-1/2} (2\pi)^{-1/4} \alpha^{(2n+1)/4} \quad (2.61)$$

arising from a potential:

$$V(r) = 2\alpha^2 r^2 + \frac{n(n-1) - l(l+1)}{2r^2} \quad (2.62)$$

α is a constant, the greatest advantageous type of these functions is the easily integrable polycentric functions. They are less satisfactory than

CHAPTER ५. THEORY

STO as representations of atomic orbitals, particularly because they do not have a cusp at the origin.

५.११ *Roothaan-Hall Equations*

Substituting the linear expansion of Eq. (५.११) in the molecular orbital integrals [५], yields:

$$H_{ii} = \sum_{\mu\nu} C_{\mu i}^* C_{\nu i} H_{\mu\nu} \quad (५.६३)$$

where $H_{\mu\nu}$ is the core Hamiltonian matrix elements,

$$H_{\mu\nu} = \int \phi_{\mu}(1) H^{\text{core}} \phi_{\nu}(1) d\tau_1 \quad (५.६४)$$

Similarly we may write

$$J_{ij} = \sum_{\mu\lambda\nu\sigma} C_{\mu i}^* C_{\lambda j}^* C_{\nu i} C_{\sigma j} (\mu\nu/\lambda\sigma) \quad (५.६५)$$

$$K_{ij} = \sum_{\mu\lambda\nu\sigma} C_{\mu i}^* C_{\lambda j}^* C_{\nu i} C_{\sigma j} (\mu\lambda/\nu\sigma) \quad (५.६६)$$

where $(\mu\nu/\lambda\sigma)$ is the differential overlap matrix elements

$$(\mu\nu/\lambda\sigma) = \iint \phi_{\mu}(1) \phi_{\nu}(1) \frac{1}{r_{12}} \phi_{\lambda}(2) \phi_{\sigma}(2) d\tau_1 d\tau_2 \quad (५.६७)$$

The total electronic energy of Eq. (५.१३) can be written in terms of integral over atomic orbitals. By substituting the pervious expressions in the equation of the electronic energy, we obtain

$$\varepsilon = \sum_{\mu\nu} P_{\mu\nu} H_{\mu\nu} + \frac{1}{2} \sum_{\mu\nu\lambda\sigma} P_{\mu\nu} P_{\lambda\sigma} [(\mu\nu/\lambda\sigma) - \frac{1}{2}(\mu\lambda/\nu\sigma)] \quad (५.६८)$$

where $P_{\mu\nu}$ is the density matrix elements,

CHAPTER 7. THEORY

$$P_{\mu\nu} = 2 \sum_i^{\text{occ}} C_{\mu i}^* C_{\nu i} \quad (7.69)$$

Applying the variational method to Eq. (7.68), a small variation of the molecular orbital ψ_i can now be given as

$$\delta\psi_i = \sum_{\mu} \delta C_{\mu i} \phi_{\mu} \quad (7.70)$$

And when applying the condition for a stationary point ($\delta\varepsilon = 0$), one can obtain the following final form, [77, 83, 84]

$$\sum_{\nu} (F_{\mu\nu} - \varepsilon_i S_{\mu\nu}) C_{\nu i} = 0 \quad (7.71)$$

where $F_{\mu\nu}$ is the Fock matrix

$$F_{\mu\nu} = H_{\mu\nu} + \sum_{\lambda\sigma} P_{\lambda\sigma} \left((\mu\nu/\lambda\sigma) - \frac{1}{2} (\mu\lambda/\nu\sigma) \right) \quad (7.72)$$

The equations for LCAO which self-consistent field molecular orbitals, Eq. (7.71) are algebraic equations rather than differential equations (Hartree-Fock equations). They were set forth independently by Hall and by Roothaan, These equations are solved by first assuming an initial set of linear expansion coefficients $C_{\mu i}$, generating the density matrix $P_{\mu\nu}$ and computing the first guess at $F_{\mu\nu}$, then one can calculate a new matrix of $C_{\mu i}$. This procedure is continued until there is no change in $C_{\mu i}$ between iterations [7].

7.1.2 Semi-empirical Methods

The approach which involves solving the HF equations with a few other short-cuts as possible is called ab initio method [84, 85]. Because everything is calculated based on simple physics, we can say that the

CHAPTER 7. THEORY

results are "from first principles". This method involves the evaluation of large number of two electron integrals. For the large systems the evaluation of two electron integrals becomes a computer time problem. The most widely used methods are the semi-empirical methods [10]. These methods are based on the observation that vast majority of computer time is spent dealing with integrals. The zero-differential overlap approximation (ZDOA) is the starting point for many semi-empirical methods [7, 11].

The ZDOA sets all but a few terms in the differential overlap matrix identically to zero:

$$(p\mu\nu/\lambda\sigma) = (p\mu\mu/\lambda\lambda)\delta_{\mu\nu}\delta_{\lambda\sigma} \quad (7.73)$$

and the overlap integrals, $S_{\mu\nu}$ are neglected in the normalization of the molecular orbitals. The Hamiltonian matrix elements $H_{\mu\nu}$, are treated semi-empirically.

The ZDOA simplifies the Roothaan equations to become:

$$\sum_{\nu} F_{\mu\nu} C_{\nu i} = \epsilon_i C_{\mu i} \quad (7.74)$$

$$F_{\mu\nu} = \begin{cases} H_{\mu\mu} - \frac{1}{2} P_{\mu\mu} (p\mu\mu/\mu\mu) + \sum_{\lambda} P_{\lambda\lambda} (p\mu\mu/\lambda\lambda) & \nu = \mu \\ H_{\mu\nu} - \frac{1}{2} P_{\mu\nu} (p\mu\mu/\nu\nu) & \mu \neq \nu \end{cases} \quad (7.75)$$

These equations are only applied to the closed shell molecules and reduce the number of 2-electron integrals.

7.12.1 Complete Neglect of Differential Overlap (CNDO)

The degree to which the ZDOA is applied varies from one method to another. The simplest form is the complete neglect of differential

CHAPTER ۷. THEORY

overlap (CNDO) [۱۹,۲۰] introduced by Pople, Santry and Segal. Only valence electrons are treated explicitly, the inner shells being treated as part of a rigid core. The remaining ۷-electron integrals in this approximation is given by:

$$(\mu\mu/vv) = \gamma_{AB} \quad (۷.۷۶)$$

where γ_{AB} is the average electrostatic repulsion between any electron on atom A and any electron on atom B. Therefore, the integral depends only on the nature of the atoms A&B.

The Fock matrix elements for this approximation is given as:

$$F_{\mu\nu} = \left\{ \begin{array}{ll} H_{\mu\mu} - \frac{1}{2}P_{\mu\mu}\gamma_{AA} + \sum_B P_{BB}\gamma_{AB} & \nu = \mu, \phi_{\mu} \text{ on atom A} \\ H_{\mu\nu} - \frac{1}{2}P_{\mu\nu}\gamma_{AB} & \nu \neq \mu, \phi_{\mu} \text{ on A, } \phi_{\nu} \text{ on B} \end{array} \right\} \quad (۷.۷۷)$$

where P_{BB} is the total electronic density associated with atom B,

$$P_{BB} = \sum_{\lambda}^B P_{\lambda\lambda} \quad (۷.۷۸)$$

we can apply the same approximation to the matrix elements $H_{\mu\nu}$ of the core Hamiltonian operator,

$$H = -\frac{1}{2}\nabla^2 - \sum_B V_B \quad (۷.۷۹)$$

where $-V_B$ is the potential due to the nucleus and inner shells of atom B. Thus one arrives at:

CHAPTER 7. THEORY

$$H_{\mu\nu} = \left\{ \begin{array}{ll} U_{\mu\mu} - \sum_{B \neq A} (\mu/V_B / \mu), & \nu = \mu, \phi_\mu \text{ on A} \\ U_{\mu\nu} - \sum_{B \neq A} (\mu/V_B / \nu), & \phi_\mu, \phi_\nu \text{ on A} \\ (\mu / -\frac{1}{2}\nabla^2 - V_A - V_B / \nu) - \sum_{C \neq A, B} (\mu/V_C / \nu) & \phi_\mu \text{ on A, } \phi_\nu \text{ on B} \end{array} \right\} \quad (7.80)$$

Where

$$U_{\mu\nu} = (\mu / -\frac{1}{2}\nabla^2 - V_A / \nu) \quad (7.81)$$

We shall restrict ourselves to the s, p, d, sets in the following development. If we use these sets, $U_{\mu\nu}$, when $\mu \neq \nu$, is zero by symmetry. The term $(\mu/V_B / \mu)$ must be a constant (V_{AB}), where $-V_{AB}$ is the interaction of any valence electron on atom A with the core of atom B. Furthermore, neglecting the monatomic differential overlap means that $(\mu/V_B / \nu) = 0, \mu \neq \nu$. For $H_{\mu\nu}$, when μ on A and ν on B the second part is neglected in Eq. (7.80) because it is a three-center integral. The first part of this equation is a measure of the possible lowering of energy levels by an electron being in the electrostatic field of two atoms simultaneously. It is referred to as a resonance integral $\beta_{\mu\nu}$, which is assumed to be proportional to the overlap integral,

$$\beta_{\mu\nu} = \beta_{AB}^0 S_{\mu\nu} \quad (7.82)$$

Applying these further conditions to Eq.(7.80), we arrive at

$$H_{\mu\nu} = \left\{ \begin{array}{ll} U_{\mu\mu} - \sum_{B \neq A} V_{AB}, & \mu = \nu, \phi_\mu \text{ on A} \\ 0, & \mu \neq \nu, \phi_\mu, \phi_\nu \text{ both on A} \\ \beta_{AB}^0 S_{\mu\nu} & \mu \neq \nu, \phi_\mu \text{ on A, } \phi_\nu \text{ on B} \end{array} \right\} \quad (7.83)$$

This expression can now be substituted into the Fock matrix,

CHAPTER ५. THEORY

$$F_{\mu\mu} = U_{\mu\mu} + (P_{AA} - \frac{1}{2}P_{\mu\mu})\gamma_{AA} + \sum_{B \neq A} [-Q_B\gamma_{AB} + (Z_B\gamma_{AB} - V_{AB})] \quad (५.८६)$$

$$F_{\mu\nu} = \beta_{AB}^0 S_{\mu\nu} - \frac{1}{2}P_{\mu\nu}\gamma_{AB} \quad \mu \neq \nu \quad (५.८७)$$

where Q_B is the net charge on atom B,

$$Q_B = Z_B - P_{BB} \quad (५.८८)$$

The quantity $Z_B\gamma_{AB} - V_{AB}$ represents the difference between the potentials due to the valence electrons and core of the neutral atom B. The total energy can be written by applying these approximations

$$E_{\text{tot}} = \frac{1}{2} \sum_{\mu\nu} P_{\mu\nu} (H_{\mu\nu} + F_{\mu\nu}) + \sum_{A < B} Z_A Z_B R_{AB}^{-1} \quad (५.८९)$$

To evaluate $S_{\mu\nu}$, $U_{\mu\nu}$, V_{AB} , γ_{AB} and β_{AB}^0 we can use two systems adopted, termed CNDO/1 and CNDO/2 [५, ६५].

१. CNDO/1

- The overlap integrals are directly evaluated using formulas discussed in appendix A.

γ_{AB} is calculated as the two center coulomb integral involving valence s functions,

$$\gamma_{AB} = \iint s_A^2(1)(r_{12})^{-1} s_B^2(2) d\tau_1 d\tau_2 \quad (५.९०)$$

The evaluation of these integrals is also discussed in appendix B.

- The electron-ion interaction V_{AB} is also calculated using an s-orbital on atom A.

CHAPTER ५. THEORY

$$V_{AB} = Z_B \int s_A^2(\mathbf{r}_{1B})^{-1} d\tau_1 \quad (५.८१)$$

- The one-electron Hamiltonian matrix elements, $U_{\mu\mu}$, is obtained by fitting to atomic ionization energies.
- The bonding parameters β_{AB}° are approximated by the expression

$$\beta_{AB}^{\circ} = \frac{1}{2}(\beta_A^{\circ} + \beta_B^{\circ}) \quad (५.९०)$$

Here β_A depends only on the nature of atom A, so only semi-empirical parameter is selected for each element.

५. CNDO/५

This version of the CNDO method differs from CNDO/१ in the way that handles penetration integrals and the one center atomic core integrals. There are two improvements made to the CNDO/१ parameterization.

१. The electron-core potential integrals V_{AB} are no longer evaluated separately but are related to the electron repulsion integrals by

$$V_{AB} = Z_B \gamma_{AB} \quad (५.९१)$$

५. Instead of fitting the $U_{\mu\mu}$ using only ionization potential, an average of the ionization potential and electron affinities is used,

$$-\frac{1}{2}(I_{\mu} + A_{\mu}) = U_{\mu\mu} + (Z_A - \frac{1}{2})\gamma_{AA} \quad (५.९२)$$

where I_{μ}, A_{μ} are the ionization potential and electron affinities respectively. This should make CNDO/५ better suited to modeling the tendencies for atomic orbitals to both gain and lose electrons than CNDO/१.

CHAPTER 2. THEORY

2.1.2 Intermediate Neglect of Differential Overlap (INDO)

When two electrons in different atomic orbitals on the same atom have a smaller average repulsion energy if they have parallel spins, the exchange integral of this type is given by

$$(\mu\nu/\mu\nu) = \iint \phi_\mu(1)\phi_\mu(2) \frac{1}{r_{12}} \phi_\nu(1)\phi_\nu(2) d\tau_1 d\tau_2 \quad \mu \neq \nu \quad (2.93)$$

In CNDO theory such integrals are neglected, and all interaction between two electrons on atom A are replaced by γ_{AA} irrespective of their spin. In this method the exchange integral of this type is taken into account.

The diagonal Fock matrix element in INDO [71] is

$$F_{\mu\mu} = U_{\mu\mu} + \sum_{\lambda}^A P_{\lambda\lambda} [(\mu\mu/\lambda\lambda) - \frac{1}{2}(\mu\lambda/\mu\lambda)] + \sum_{A \neq B} (P_{BB} - Z_B) \gamma_{AB} \quad \mu \text{ on A} \quad (2.94)$$

$$F_{\mu\nu} = P_{\mu\nu} \left[\frac{3}{2}(\mu\nu/\mu\nu) - \frac{1}{2}(\mu\mu/\nu\nu) \right] \quad \mu \neq \nu \text{ both on A} \quad (2.95)$$

$$F_{\mu\nu} = \frac{1}{2}(\beta_A^0 + \beta_B^0) S_{\mu\nu} - \frac{1}{2} P_{\mu\nu} \gamma_{AB} \quad \mu \text{ on A, } \nu \text{ on B} \quad (2.96)$$

For γ_s and γ_p orbitals which have the same radial parts. The non vanishing integrals are given by Slater [72]

$$(ss/ss) = (ss/xx) = F^0 = \gamma_{AA} \quad (2.97)$$

$$(sx/sx) = \left(\frac{1}{3}G^1\right) \quad (2.98)$$

$$(xy/xy) = \frac{3}{25}F^2 \quad (2.99)$$

$$(xx/xx) = F^0 + \frac{4}{25}F^2 \quad (2.100)$$

$$(xx/yy) = F^0 - \frac{2}{25}F^2 \quad (7.1.1)$$

and similar expressions for (ss/zz), ... etc.

where F^0, G^1 and F^2 are two-electron integrals involving the radial parts of the atomic orbitals. All the above integrals are one-center integrals. By one-center integrals we mean that the integrated functions are on one atom. These integrals will be discussed in appendix B. Two-center integrals mean that the integrated functions are distributed on two atoms. For the large atomic number such as tin ($Z=82$), the evaluation of these two-electron integral is impossible because the relativistic effects will affect the energy levels which is used to evaluate these integrals. However, we can evaluate these integrals from theoretical definition as explained in appendix A.

7.1.3 Tight-Binding Method (TBM)

Up to now we can not apply ab initio or approximate self-consistent theories to solids because of the infinite number of atoms and electrons in the solid. Therefore, in this method we can apply the linear combination of atomic orbitals to the solids as following.

Consider a microcrystal of N^3 large unit cells each containing η spin orbitals. The total number of electrons in the system is $\tilde{N} = \eta N^3$, and the total electronic wavefunction Φ with the Hartree-Fock approximation can be represented as a single determinate of \tilde{N} order [73]

$$\Phi(1, \dots, \tilde{N}) = \tilde{\lambda} |\psi_1(\mathbf{k}, \mathbf{r}) \dots \psi_\alpha(\mathbf{k}, \mathbf{r}) \dots \psi_{\tilde{N}}(\mathbf{k}, \mathbf{r})| \quad (7.1.2)$$

CHAPTER 3. THEORY

where $\psi_\alpha(\mathbf{k}, \mathbf{r})$ is the crystal orbital, \mathbf{k} denotes the wave vector, \mathbf{r} is a position vector and λ is the normalization constant. In constructing one-electron crystal orbital $\psi_\alpha(\mathbf{k}, \mathbf{r})$ we need the following properties

1. The translational symmetry of the crystal where by the crystal orbital is described by Bloch theorem [3].

$$\psi_\alpha(\mathbf{k}, \mathbf{r}) = U(\mathbf{k}, \mathbf{r}) \exp(i\mathbf{k} \cdot \mathbf{r}) \quad (3.1.3)$$

with $U(\mathbf{k}, \mathbf{r})$ having the periodicity of the crystal

$$U(\mathbf{k}, \mathbf{r}) = U(\mathbf{k}, \mathbf{r} + \mathbf{R}_u) \quad (3.1.4)$$

where (\mathbf{R}_u) is the position vector defined as

$\mathbf{R}_u = n_x \mathbf{a}_x + n_y \mathbf{a}_y + n_z \mathbf{a}_z$; n_x, n_y, n_z are integers and $\mathbf{a}_x, \mathbf{a}_y$ and \mathbf{a}_z are the basic translation vectors of the large unit cell (LUC) of the crystal. The crystal orbital is translated to the new position $\mathbf{r} + \mathbf{R}_u$, then we have

$$\psi(\mathbf{k}, \mathbf{r} + \mathbf{R}_u) = U(\mathbf{k}, \mathbf{r} + \mathbf{R}_u) \exp(i\mathbf{k} \cdot (\mathbf{r} + \mathbf{R}_u)) \quad (3.1.5)$$

Using the Bloch condition in equation (3.1.3) we obtain

$$\psi(\mathbf{k}, \mathbf{r} + \mathbf{R}_u) = \psi_\alpha(\mathbf{k}, \mathbf{r}) \exp(i\mathbf{k} \cdot \mathbf{R}_u) \quad (3.1.6)$$

2. The wavefunction should be repeated after N cells [3], i.e.

$$\psi_\alpha(\mathbf{k}, \mathbf{r} + N) = \psi_\alpha(\mathbf{k}, \mathbf{r}) \quad (3.1.7)$$

Thus, the Bloch orbital is approximated by a linear combination of one-electron molecular orbitals X_u in the cells. Hence

$$\psi_\alpha(\mathbf{k}, \mathbf{r}) = \sum_u^{\text{cells}} \exp(i\mathbf{k} \cdot \mathbf{R}_u) X_u(\mathbf{k}, \mathbf{r} - \mathbf{R}_u) \quad (3.1.8)$$

CHAPTER 7. THEORY

The one electron molecular orbital may be written as a LCAO of atomic orbitals in the cell:

$$X_u(k, r - R_u) = \sum_p^{\text{basis}} C_{p\alpha}(k) \phi_p(r - R_u) \quad (7.109)$$

where ϕ_p is the basis function. The one electron crystal orbital is written as

$$\psi_\alpha(k, r) = \sum_u^{\text{cells}} \sum_p^{\text{basis}} \exp(ik \cdot R_u) C_{p\alpha}(k) \phi_p(r - R_u) \quad (7.110)$$

The total Hamiltonian for a microcrystal consisting of \tilde{N} electrons may be written as,

$$H = \sum_\alpha^{\tilde{N}} \left(-\frac{1}{2} \nabla_\alpha^2 - \sum_a^{n_a} Z_a r_{a\alpha}^{-1} \right) + \frac{1}{2} \sum_\alpha^{\tilde{N}} \sum_\beta^{\tilde{N}} r_{\alpha\beta}^{-1} + \sum_a^{n_a} \sum_b^{n_b} Z_a Z_b R_{ab}^{-1} \quad (7.111)$$

The Hartree-Fock equations for the microcrystal can be written as,

$$\sum_p (F_{pq}(k) - \epsilon_\alpha(k) S_{pq}(k)) C_{p\alpha}(k) = 0 \quad (7.112)$$

where F_{pq} and S_{pq} (the Fock and overlap integrals) are now given by:

$$F_{pq}(k) = \sum_u F_{op, uq} \exp(ik \cdot R_u) \quad (7.113)$$

$$S_{pq}(k) = \sum_u S_{op, uq} \exp(ik \cdot R_u) \quad (7.114)$$

$$F_{op, uq} = \langle \phi_p(r - R_0) | H | \phi_q(r - R_u) \rangle \quad (7.115)$$

$$S_{op, uq} = \langle \phi_p(r - R_0) | \phi_q(r - R_u) \rangle \quad (7.116)$$

CHAPTER 7. THEORY

The Fock matrix elements may be expressed in terms of one and two-electron components:

$$F_{op,uq} = H_{op,uq} + G_{op,uq} \quad (7.117)$$

with

$$H_{op,uq} = \left\langle \phi_p^o(1) \left| -\frac{1}{2} \nabla_1^2 - \sum_{\alpha} Z_{\alpha} r_{1\alpha}^{-1} \right| \phi_q^u(1) \right\rangle \quad (7.118)$$

and

$$G_{op,uq} = \sum_{v,\lambda} \sum_{r,s}^{\text{all basis cells functions}} P_{rs}^{v\lambda} \left((\phi_p^o \phi_q^u | \phi_r^v \phi_s^{\lambda}) - \frac{1}{2} (\phi_p^o \phi_r^v | \phi_s^{\lambda} \phi_q^u) \right) \quad (7.119)$$

where

$$\phi_q^u \equiv \phi_q(r - \mathbf{R}_u) \quad (7.120)$$

and

$$(\phi_p^o \phi_q^u | \phi_r^v \phi_s^{\lambda}) = \langle \phi_p^o(1) \phi_r^v(2) | r_{12}^{-1} | \phi_q^u(1) \phi_s^{\lambda}(2) \rangle \quad (7.121)$$

$P_{rs}^{v\lambda}$ is a density matrix element with the form

$$P_{rs}^{v\lambda} = \sum_{\mathbf{k}'} P_{rs}(\mathbf{k}') \exp[i\mathbf{k}' \cdot (\mathbf{R}_{\lambda} - \mathbf{R}_v)] \quad (7.122)$$

with

$$P_{rs}(\mathbf{k}') = 2 \sum_{\alpha}^{\text{occ}} C_{r\alpha}^*(\mathbf{k}') C_{s\alpha}(\mathbf{k}') \quad (7.123)$$

The new wave vector \mathbf{k}' refers to the summation over all the allowed values of \mathbf{k} [73].

7.1.4 The Large Unit Cell-INDO Method

In the large unit cell method, we shall need to reduce the zone of the wave vector (k) to simplify the calculations [13]. The first Brillouin zone is defined by the wave vector with a lattice constant (a) in the one dimensional case

$$+\pi/a \geq k \geq -\pi/a$$

The zone of the wave vector will become smaller when choosing a LUC lattice with a large lattice constant and when the lattice constant of LUC lattice is equal to (γa). This zone is defined by the new wave vector

$$+\pi/2a \geq k \geq -\pi/2a$$

Thus, if we choose a LUC lattice with a lattice constant large enough will make all points in the first Brillouin zone close to the point $k=0$ in the three-dimensional case. This leads to use only the points at the origin of the first Brillouin zone in the solving of the self consistent equations. This approximation is called the $k=0$ approximation [13]. Substituting $k=0$ in Eq. (7.1.12) yields

$$\sum_p (F_{pq}(0) - \epsilon_\alpha(0)) C_{p\alpha}(0) = 0 \quad (7.124)$$

The Fock matrix elements within the LUC-INDO method have the following form:

$$F_{pp}(0) = U_{op,op} - \sum_{B \neq A} \sum_v Z_B \gamma_{AB}^{ov} + \sum_v \beta_A^o (S_{op,vp} - \delta_{ov}) + \sum_r \sum_v p_{rr}(0) \gamma_{AB}^{ov} - \frac{1}{2} \sum_{v \neq 0} P_{pp}(0) \gamma_{AA}^{ov} - \frac{1}{2} \sum_{r \text{ on } A} P_{rr}(0) (\phi_p^o \phi_r^o / \phi_p^o \phi_r^o) \quad (7.125)$$

$$F_{pq}(0) = \sum_v \beta_{AB}^o S_{op,vq} - \frac{1}{2} P_{pq}(0) \sum_v \gamma_{AB}^{ov} \quad (7.126)$$

CHAPTER 7. THEORY

for p and q on different atomic centres and

$$F_{pq}(0) = \sum_{v \neq 0} \beta_A^o S_{op,vq} - \frac{1}{2} P_{pq}(0) \sum_{v \neq 0} \gamma_{AA}^{ov} + \frac{1}{2} P_{pq}(0) [3(\phi_p^o \phi_q^o / \phi_p^o \phi_q^o) - (\phi_p^o \phi_p^o / \phi_q^o \phi_q^o)] \quad (7.127)$$

for p and q on the same atomic centre.

Evarestov [70] and Szymanski [71] added correction to previous equations by suggesting the modulating function $f(x)$

$$f(x) = \left(\frac{\sin(x)}{x} \right)^2 \quad (7.128)$$

where x for the Λ atom LUC is given by

$$x = \frac{\pi R_{AB}^{ov}}{a} \quad (7.129)$$

where R_{AB}^{ov} is the distance between the atom A at the central lattice o and the atom B at the v lattice. The modulating function is multiplied by the density matrix ($P_{\mu\nu}$) and two electron integral γ_{AB} when a summation on the LUCs (v) is made to avoid divergence when including large number of neighbors.

The final form of the Fock matrix elements within the LUC-INDO method with the added modulating function $f(x)$ is given by:

$$F_{pp}(0) = U_{op,op} - \sum_{B \neq A} \sum_v Z_B \gamma_{AB}^{ov} + \sum_v \beta_A^o (S_{op,vp} - \delta_{ov}) + \sum_r \sum_v P_{rr}(0) \gamma_{AB}^{ov} - \frac{1}{2} \sum_{v \neq 0} P_{pp}(0) f(x) \gamma_{AA}^{ov} - \frac{1}{2} \sum_{r \text{ on } A} P_{rr}(0) (\phi_p^o \phi_r^o / \phi_p^o \phi_r^o) \quad (7.130)$$

$$F_{pq}(0) = \sum_v \beta_{AB}^o S_{op,vq} - \frac{1}{2} P_{pq}(0) \sum_v f(x) \gamma_{AB}^{ov} \quad (7.131)$$

for p and q on different atomic centres and

CHAPTER 2. THEORY

$$F_{pq}(0) = \sum_{v \neq 0} \beta_A^0 S_{op,vq} - \frac{1}{2} P_{pq}(0) \sum_{v \neq 0} f(x) \gamma_{AA}^{0v} + \frac{1}{2} P_{pq}(0) [3(\phi_p^0 \phi_q^0 / \phi_p^0 \phi_q^0) - (\phi_p^0 \phi_p^0 / \phi_q^0 \phi_q^0)] \quad (2.132)$$

for p and q on the same atomic centre.

These equations are programmed to calculate the effect of pressure and temperature on some properties of grey tin crystal in the next chapter.

2.10 Corrections to the Hartree-Fock Theory

2.10.1 Correlation Corrections

The Hartree-Fock equation is an approximated solution to the true ground state many body wavefunction. Terms not included in the Hartree-Fock energy referred to as correlation contributions. Correlation energy is defined as the difference between Hartree-Fock and exact energy [37, 48].

$$E_{\text{corr}} = E_{\text{exact}} - E_{\text{HF}} \quad (2.133)$$

Correlation energies may be included by considering Slater determinates composed of orbitals which represent excited state contribution. This method of including unoccupied orbitals in the many body wavefunction is referred to as configuration interaction or "CI" [53, 66, 67]. The exact wavefunction can be expressed as a linear combination of the determinatal wavefunction:

$$\Psi = a_0 \Psi_0 + a_1 \Psi_1 + a_2 \Psi_2 + \dots \quad (2.134)$$

Where Ψ_0 is the full Hartree-Fock many-electron wavefunction. Here Ψ_1, Ψ_2, \dots are wavefunctions for other configurations, and the linear coefficient a_1, a_2, \dots are to be determined. CI theory is very expensive to implement, but the results are usually very good.

CHAPTER 7. THEORY

Another method of correlation to correct the calculated Hartree-Fock total energy that can be applied to molecular and solid calculations is the Møller-Plesset perturbation theory (MPPT) [18, 19]. Perturbation theory attempts to describe differences between systems, rather than to describe the systems separately and then takes the difference. In this method the correlation Hamiltonian is written as a perturbation over the exactly solvable Hartree-Fock Hamiltonian

$$\hat{H} = \hat{H}_0 + \lambda \hat{H}' \quad (7.130)$$

where \hat{H} is the total Hamiltonian, \hat{H}_0 is the Hartree-Fock Hamiltonian, λ is a dimensionless parameter and H' is the correction Hamiltonian. In this method \hat{H}_0 is taken to be the sum of the one-electron Fock operators,

$$\hat{H}_0 = \sum_{i=1}^n \hat{F}_i \quad (7.131)$$

The wavefunction is now given by

$$\Psi_\lambda = \Psi^{(0)} + \lambda \Psi^{(1)} + \lambda^2 \Psi^{(2)} + \dots \quad (7.132)$$

and the energy will be

$$E_\lambda = E^{(0)} + \lambda E^{(1)} + \lambda^2 E^{(2)} \quad (7.133)$$

The perturbation $H^{(1)}$ is given by

$$\hat{H}^{(1)} = \hat{H} - \sum_{i=1}^n \hat{F}_i \quad (7.134)$$

The HF energy E_{HF} associated with ground-state HF wavefunction Ψ_0 is the expectation value

CHAPTER 7. THEORY

$$E_{\text{HF}} = \langle \Psi_0 | H_0 + H^{(1)} | \Psi_0 \rangle \quad (7.1 \xi 0)$$

The zero-order energy $E^{(0)}$ and the first order energy correction $E^{(1)}$ is given as

$$E^{(0)} = \langle \Psi_0 | H_0 | \Psi_0 \rangle \quad (7.1 \xi 1)$$

$$E^{(1)} = \langle \Psi_0 | H^{(1)} | \Psi_0 \rangle \quad (7.1 \xi 2)$$

From Eqs (7.1 ξ 0)-(7.1 ξ 2) we conclude that

$$E_{\text{HF}} = E^{(0)} + E^{(1)} \quad (7.1 \xi 3)$$

The second-order contribution to the Møller-Plesset energy is

$$E^{(2)} = - \sum_{i < j}^{\text{occ}} \sum_{a < b}^{\text{virt}} (\epsilon_a + \epsilon_b - \epsilon_i - \epsilon_j)^{-1} (ij/ab)^2 \quad (7.1 \xi 4)$$

where (ij/ab) is a two-electron integral over spin orbitals,

$$(ij/ab) = \iint \psi_i^*(1) \psi_j^*(2) \left(\frac{1}{r_{12}} \right) [\psi_a(1) \psi_b(2) - \psi_b(1) \psi_a(2)] d\tau_1 d\tau_2 \quad (7.1 \xi 5)$$

Here ψ_i and ψ_j are the occupied spin orbitals, ψ_a, ψ_b virtual spin orbitals.

Eq. (7.1 ξ 4) is the final form of the second-order energy correction and the inclusion of it is designated MP2 [20, 28, 29].

It is possible to extend the MPPT to include third-and fourth-order energy corrections, and the procedures are then referred to as MP3 and MP4 respectively. The full discussion of this method can be found in the reference [30], and this method is used in this work.

CHAPTER 2. THEORY

2.1.2 Relativistic Corrections

For high atomic number (Z) nuclei, the relativistic effects [2.1, 2.2, 2.3, 2.4] can not be neglected in the band structure calculations. There are three terms of relativistic corrections which may be added to Schrödinger equation [2.4].

1. Kinetic energy correction term

$$H_1 = -\frac{P^4}{8m^3c^2} \quad (2.1.26)$$

where P and m are the momentum and mass of the particle, c the speed of light. The effect of this term on s state ($\ell = 0$) is more pronounced than the other states of high value of the angular momentum (ℓ) and this term has a negative expectation value.

2. Potential energy correction term (Darwin correction)

$$H_2 = \frac{\hbar^4}{8m^2c^2} \nabla^2 V_p \quad (2.1.27)$$

where $\hbar = h/2\pi$, V_p is the potential. This term has an effect on s states and has a positive expectation value.

3. Spin-orbital term

$$H_3 = \frac{1}{2m^2c^2} \frac{dV_p}{dr} L \cdot S \quad (2.1.28)$$

where L is the angular momentum operator and S is the spin operator. This term has no effect on s state ($\ell = 0$) and has the effect of splitting levels of $\ell \neq 0$. The splitting of the p states can be measured directly in experiment. The experimental spin-orbit splitting (Δ_0) of the p states at the top of the valence band of the grey tin (dealing with solid in our

CHAPTER 7. THEORY

work) is equal to (0.1 eV) [10]. As an example of this effect Γ_{25} point is splitted to Γ_8^+ and Γ_7^+ states as follows

$$E(\Gamma_8^+) = E(\Gamma_{25}) + \lambda \quad (7.149)$$

$$E(\Gamma_7^+) = E(\Gamma_{25}) - 2\lambda \quad (7.150)$$

where λ is given by

$$\lambda = \frac{\Delta_0}{3}$$

The experimental estimation of the effect of the first and two terms is difficult, but the inclusion of these terms in any calculations is easier than the inclusion of spin-orbit term. This is so because the number of states will be increased when the spin-orbit term is added to the Hamiltonian. The preferred corrections include the relativistic correction to the kinetic and potential energy only and to drop the spin-orbit term from the calculations [13].

3.1 The Structure of Computer Program

In Fig (૩.૧), a block diagram of the computational procedure used in the present calculations is shown. Each individual program step serves to perform a specific task as in the following:

૧. Specification of the positions of atoms and the kind of states that are given as input data.
૨. The (overlap, core Hamiltonian and two electron) integrals are calculated and stored.
૩. The Fock matrix F_{pq} is calculated from an initial guess of the wavefunction with the calculated integrals in the previous step.
૪. Calculation of the density matrix from the new eigenvalues.
૫. Calculation of the total electronic energy from the density matrix.
૬. Calculation of a new Fock matrix from the new eigenvalues.
૭. Steps ૪ and ૫ are repeated until self-consistency is achieved.
૮. The total energy compared with the previous one and when the total energy differs from the preceding one by more than a given tolerance, steps ૬, ૪ and ૫ are repeated. If the final total energy differs from the preceding one by less than the given tolerance, step ૯ is executed.
૯. Calculation of the correlation corrections and correlated wavefunctions using the final HF wavefunction.
૧૦. Calculation of the band structure, some physical properties of (α -Sn) and the effect of pressure and temperature on these properties.

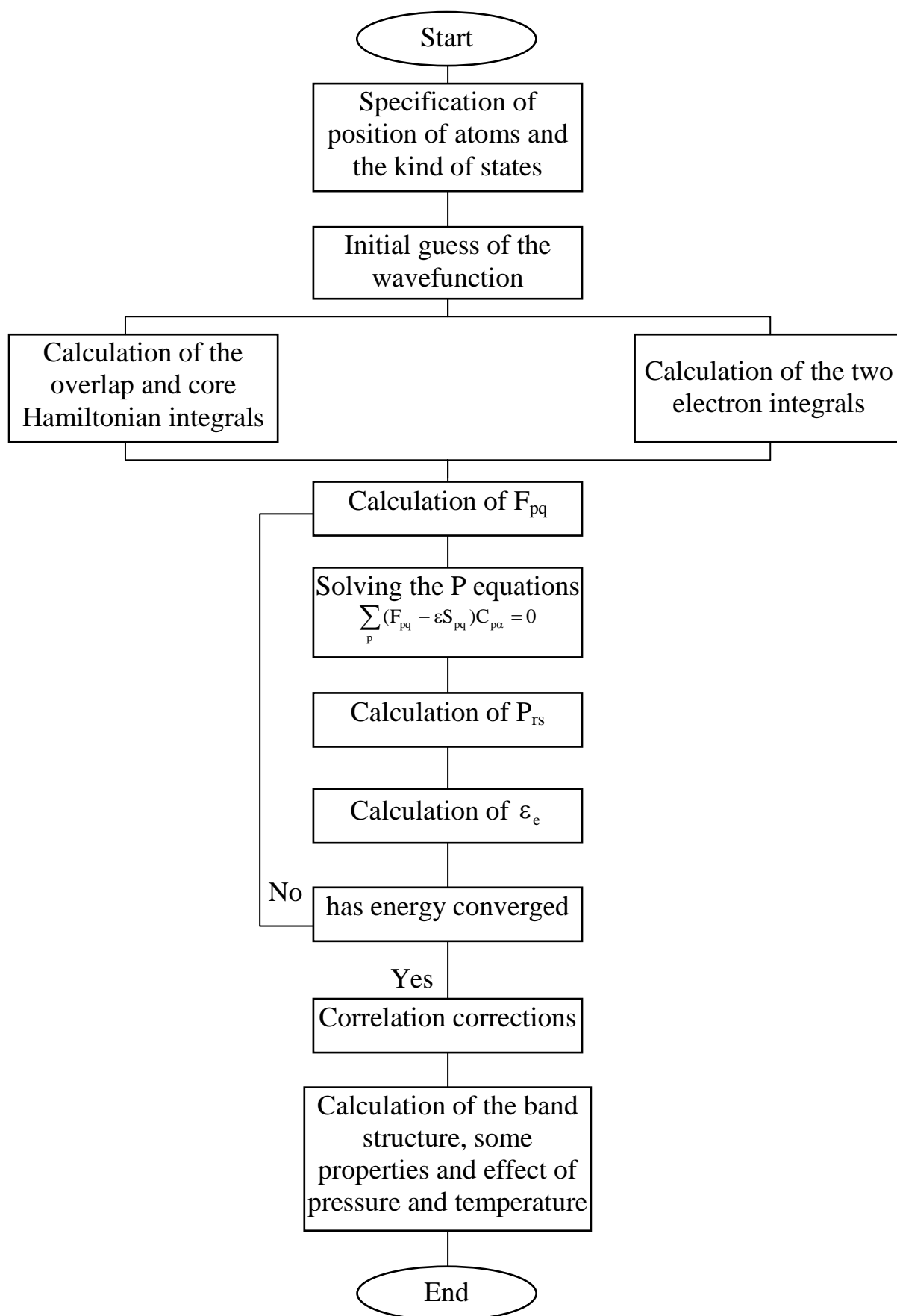


Fig (૩.૧): The flow chart of computer program used to calculate the band structure and some physical properties of $(\alpha - S_n)$ and the effect of pressure and temperature on these properties.

૩.૩ Choice of Large Unit Cell

The general approach to the selection of a large unit cell, such that those special points required in the Brillouin zone occur at the $\Gamma(\vec{K}=0)$ points in the reduced Brillouin zone [૧૧]. For a face-centered cubic lattice system, large unit cells can be based on either the primitive translation vector set [૩૧].

$$\bar{a}_1 = \frac{a_0}{2} (1,1,0)$$

$$\bar{a}_2 = \frac{a_0}{2} (1,0,1)$$

$$\bar{a}_3 = \frac{a_0}{2} (0,1,1)$$

or on the Bravais translation set:

$$\bar{a}_1 = a_0 (1,1,0)$$

$$\bar{a}_2 = a_0 (1,0,1)$$

$$\bar{a}_3 = a_0 (0,1,1)$$

Calculations on LUCs are centered on small and limited number of atoms per a LUC. In Table (૩.૧) the most common LUCs that are used for the calculations of the band structure of diamond structure crystal are listed with the high symmetry points that are obtained from the solution of Hartree-Fock equations for these crystals [૧૩,૩૧].

Table (૨.૧): The high symmetry points for different numbers of atoms per LUCs [૧૩,૨૦].

Number of atoms in the LUC	High symmetry points
૮	$\Gamma, 3X$
૧૬	$\Gamma, 3X, 4L$
૬૪	$\Gamma, 3X, 4L, 6\Delta, 6W, 12\Sigma$
૧૨૮	$\Gamma, 3X, 4L, 6\Delta, 6W, 12\Sigma$ and ૩૨ inner points of Brillouin zone

In this work we choose the LUC of eight atoms with the diamond structure. The calculations are carried by forming a cube of a side $\sqrt[3]{a}$ where a is the lattice constant of the Bravais lattice. The number of Bravais lattices in this cube is $\sqrt[3]{V}$ lattices. The interaction of the atoms in the central Bravais lattice with the surrounding atoms up to the fourth neighbors is included. These calculations require the determination of wavefunctions and positions of 864 electrons and 216 nuclei.

૨.૨ Choice of Parameters

There are four parameters in the LUC-INDO methods. These are $\xi, \beta^o, \frac{1}{2}(I_s + A_s)$ and $\frac{1}{2}(I_p + A_p)$. In order to compensate the errors caused by neglecting many smaller integrals, empirical parameters are calibrated against reliable experimental or theoretical reference data. It is necessary to vary these parameters in order to get optimum results in the intermediate neglect of differential overlap.

CHAPTER ૩. COMPUTATIONS AND RESULTS

These parameters are varied firstly to give nearly the exact values of the equilibrium lattice constant, cohesive energy, direct band gap and valence band width. The remaining of the output data of the programs is a result of the theory that is used in the present work. We found that the investigated properties were sensitive to the aforementioned parameters. The optimum values of these parameters lead to results in agreement with the experimental results are listed in Table (૩.૫).

Table (૩.૫): Parameters set for the LUC-INDO method used in the present work

The parameter	This work
ζ (a.u. ⁻¹)	1.9960
β^0 (eV)	-0.3340
$-1/2(I_S+A_S)$ (eV)	9.402
$-1/2(I_P+A_P)$ (eV)	0.632

૩.૬ The Total Energy

By using the procedure in Fig (૩.૧), the total energy of the crystal is calculated. The process of the calculation depends on the self-consistent style. The total energy is calculated from the initial guess of the wavefunction. The new wavefunction gives a new value of the total energy. This process is continued until the difference between the last value of the total energy and the previous one is less than a given tolerance.

The tolerance of convergence of the total energy depends on whether double precision (16 digits) calculations are used or single precision (8 digits). This precision is taken as 9.0×10^{-1} (a.u) which is

CHAPTER 3. COMPUTATIONS AND RESULTS

equivalent to (0.0002 eV) . Table (3.3) shows the successive total energy calculated in each iteration without taking the correlation corrections into account. The difference of total energy between step ϕ and step ξ is $(2.8 \times 10^{-7} \text{ (a.u)})$ which is less than the required tolerance $(9 \times 10^{-7} \text{ (a.u)})$, so the calculations are terminated at step ϕ . A large number of iterations will result in an accumulation of computational errors in the matrices of the calculated quantities. Therefore, we stopped at step ϕ . In our calculation we added the correlation corrections. Since we have 32 eigenvalues of half filled with electrons, the full number of the possible configurations is $207 (16^2 + 1)$. All of these configurations are considered in the present calculations using Møller-Plesset perturbation theory discussed in section (2.10.1).

Table (3.3): The successive total energy calculated in each iteration in the present work.

Iteration no.	Total energy (a.u)
0	-28.20870.40
1	-28.23713986
2	-28.240.9289
3	-28.240.39.99
4	-28.240.42.66
5	-28.240.42304

The total energy of the crystal has a minimum value at the equilibrium lattice constant as shown in Fig (3.2). The equilibrium lattice constant is at the bottom of the total energy curve and its value is in good agreement with the experimental value as shown in Table (3.4).

Fig (૩.૨): Total energy of $(\alpha - \text{Sn})$ as a function of lattice constant after taking the correlation corrections into account.

૩.૭ The Cohesive Energy

The cohesive energy is calculated from the total energy of the large unit cell. Since the large unit cell is composed of 8 atoms, the cohesive energy is given by [૧૩]

$$E_{\text{coh}} = E^T / 8 - E_{\text{free}} - E_0 \quad (૩.૧)$$

Where E_{free} is the free atoms sp shell energy. Its value is equal to (૧૩.૨૧૨ eV) for tin [૧૬].

E_0 is the vibrational energy of ground state. Its value is (૦.૦૩ eV) [૧૧].

The calculated value of the cohesive energy is in good agreement with the experimental value as shown in Table (૩.૬). The relation between the cohesive energy and the lattice constant is shown in Fig (૩.૩).

Fig (૩.૩): Cohesive energy of $(\alpha - \text{Sn})$ as a function of lattice constant in the present work.

૩.૮ Band Structure

The band structure and the electronic properties of grey tin crystal are calculated by using the procedure of section (૩.૧). These are listed in table (૩.૬) in comparison with other results [૧૬]. It is interesting to note the effect of INDO and correlations corrections on CNDO calculations. This is shown in Table (૩.૭) using our parameter set. It can be noted that

CHAPTER ٣. COMPUTATIONS AND RESULTS

the effect of INDO or INDO + correlation corrections are in the same direction in some of the listed properties and in opposite direction in the others. It is obvious that the value of the cohesive energy determined by INDO + correlation corrections is in good agreement with the experimental value, whereas the cohesive energy value evaluated from CNDO method differs markedly from the experimental value. By using INDO and correlation corrections the hybridization state tends to increase the s state occupancy. The eigenvalues of the high symmetry points are shown in Table (٣.٦). The high symmetry Γ and X points which are listed in this table are explained in section (١.٦).

Table (٣.٤): The band structure and electronic properties of grey tin crystal in the present work compared with other results [١٤] and experimental data.

The property	Ref [١٤]	This work	Exp.
Lattice constant (a.u)	١٢.٢١	١٢.٢٦٣	١٢.٢٦٣ [١٦]
Cohesive energy (eV/atom)	٠.١	٣.١٤٤	٣.١٤ [٣]
Valence band width (eV)	١٦.٠	١١.٨٧	----
Direct band gap (eV)	٢.٦	١.٧٦ ^a	-٠.١ ^a [٧٨]
Conduction band width (eV)	----	٥.٢	-----
Hybridization state	----	$s^{١.٣٧} p^{٢.٦٣}$	-----
Neighbors included	----	٤	-----

^a Spin-orbit corrected

CHAPTER 7. COMPUTATIONS AND RESULTS

Table (7.5): The band structure and electronic properties of grey tin crystal using the parameters of the present work for CNDO calculations and for INDO and INDO+correlation corrections.

The property	CNDO	INDO	INDO +Correlation
Cohesive energy (eV/atom)	8.96	2.87	3.14
Valence band width (eV)	11.21	12.04	11.87
Direct band gap (eV)	2.33	1.0	1.76
Conduction band width (eV)	4.09	0.4	0.2
Hybridization state	$s^{1.31} p^{2.69}$	$s^{1.36} p^{2.64}$	$s^{1.37} p^{2.63}$

Table (7.6): Energy bands of grey tin crystal in eV at Γ and X high symmetry points compared with other results [14], and with the experimental data for some of these high symmetry points.

Symmetry points	Ref [14]	This work	Exp.
Γ_1	-16.0	-12.04	-----
X_{1v}	-11.2	-7.08	-----
X_{4v}	-3.9	-2.8	-----
Γ_{γ_0}	0.0	0.0	0.0
Γ_2	2.6	1.0	-0.1 ^a [78]
X_{1c}	4.39	4.37	-----
X_{4c}	10.1	7.92	-----
Γ_{γ_0}	7.6	0.19	2.6 [79]

૩.૧ Valence Electronic Charge Densities

The charge density for each valence band can be written as [૩]

$$\rho_n(\mathbf{r}) = \sum_k |\Psi_{n,k}(\mathbf{r})|^2 \quad (૩.૧)$$

Where the summation is over all states in the Brillouin zone for a given band n . The total charge density can be obtained by adding the charge density from all valence bands, that is

$$\rho(\mathbf{r}) = \sum_n \rho_n \quad (૩.૨)$$

Where the sum is over all the occupied bands. The total charge density can be calculated as the expectation value of the charge density operator $\sum_i \delta(\mathbf{r} - \mathbf{r}_i)$ [૩].

$$\rho(\mathbf{r}) = \left\langle \Psi \left| \sum_i \delta(\mathbf{r} - \mathbf{r}_i) \right| \Psi \right\rangle \quad (૩.૩)$$

In our work using the LCAO molecular orbitals wavefunctions, this may be written as

$$\rho(\mathbf{r}) = \sum_p \sum_q P_{pq} \phi_p(\mathbf{r}) \phi_q(\mathbf{r}) \quad (૩.૪)$$

The charge density for each directions in the crystal can be calculated. Figs. (૩.૫), (૩.૬) and (૩.૭) shows the charge density in the directions $[100]$, $[110]$ and $[111]$ respectively.

CHAPTER ౪. COMPUTATIONS AND RESULTS

4.1 Discussion of the Results

4.1.1 The Empirical Parameters

The value of the parameter $\frac{1}{2}(I_s + A_s)$ of the solid in the present work is less than the same value of the free atom [13], this means that the electrons of s orbitals of the solid are less connected to their atoms than in free atom. The value of the parameter $\frac{1}{2}(I_p + A_p)$ in solid is always greater than the value of the same parameter of atom. The difference between these values of parameters for solid and atom is a result of the solid formation requirements for the electrons to change their position to more convenient positions at the half distance between two neighboring atoms in a solid. Therefore, the difference between $\frac{1}{2}(I_s + A_s)$ and $\frac{1}{2}(I_p + A_p)$ is always less than the difference between these two parameters in the case of atom. On the other hand, the value of the bonding parameter β^0 of the solid is larger than that for molecule which is given by Boca [16]. This can be understood by noting that the number of bonds in solid is higher, thus the interaction energy is distributed over all these bonds while in the molecular case this energy is limited in its number and direction distribution. The value of the orbital exponent determines the charge distribution of electrons around the nucleus or in the solid. The value of this parameter for solid is larger than that for atom. This indicates the contracted charge distribution for solid and the diffuse charge distribution for atom [13].

4.1.2 The Total Energy

The parameters $\zeta, \beta^{\circ}, \frac{1}{2}(I_s + A_s)$ and $\frac{1}{2}(I_p + A_p)$ are varied till we obtain the correct minimum value of the total energy at the experimental lattice constant. The variation of these parameters is made after adding the correlation correction. The value of the total energy of the crystal is minimum at the equilibrium lattice constant and this value increases under the effect of pressure and temperature. The crystal potential is responsible for the variation of the total energy. Therefore, we notice that when the lattice constant of the crystal decreases with the increase of the compressive stress, the repulsion between electrons will increase and this increases the value of the total energy. On the other hand, as the lattice constant is larger than the equilibrium distance, the value of the total energy will be higher because the attraction between the electrons and nuclei decreases, this occurs at the effect of tensile stress and temperature.

4.1.3 The Cohesive Energy

As is obvious from Eq. (3.1), a correct calculated value of the total energy gives a correct value of the cohesive energy. This leads to that the calculated value of the cohesive energy is in good agreement with experiment results. On the other hand, the calculated value of the cohesive energy is directly proportional to the value of the total energy, thus the change in the cohesive energy is similar to the change in the total energy under the effect of compressive stress, tensile stress and temperature.

4.1.4 The Direct Band Gap

The calculated value of the direct band gap is greater than the experimental value. This is the same as in the result of other Hartree-Fock calculations [14]. The larger value of the band gap can be attributed to the approximations involved in HF method as well as in the present LUC-INDO formalism. The important approximations are:

- (a) The use of equal ζ and β^o values for s and p wavefunctions. The difference between bonding and anti-bonding state is directly proportional to $\beta^o S$, where the overlap integral S is a function of ζ . Therefore, the value of percentage difference in ζ between s and p orbitals is 14.4% for tin [16]. Thus, this difference makes an error in the band gap.
- (b) Neglecting the core states will also result in a neglect of its effects on the distribution of the outer valence electrons. The effect of core states increases in the high Z elements, so the error in the band gap increases.

We found that the band gap increases with the increase of the compressive stress. Generally, the changes in energy bands can be understood by noting the changes in the energy value of high symmetry points. The direct band gap is bound by the states $\Gamma_2 - \Gamma_{25}$. From the definition of the symmetry points, Γ_2 moves up with the decrease of the lattice constant, thus the increasing of the Γ_2 state will increase the band gap. This is in excellent agreement with Bassani and Liu [17]. They have decreased the lattice constant (a) of grey tin in their calculations by an amount 0.016a and have found that relative to Γ_{25} , the state Γ_2 moves up by ~ 0.08 Ry. We found that the reverse is true for the effect of tensile

CHAPTER 4. DISCUSSION, CONCLUSIONS AND SUGGESTIONS

stress and temperature. The decreasing of the band gap, in this case, is due to the movement of Γ_2 down when increasing the lattice constant of the crystal. The experimental results for the effect of pressure and temperature on this property for tin crystal are not available. But for other semiconductors such as Ge, GaP, GaAs, GaSb, InP, ZnSe and CdS, the experimental results have shown that the energy gaps of these semiconductors increase with increasing the pressure and decrease with increasing the temperature [14, 15].

4.1.5 The Valence and Conduction Band Width

The experimental values of these bands are not available. The valence band width can be calculated from $\Gamma_1 - \Gamma_{25}$ and the conduction band width from $\sim X_{\epsilon_c} - \Gamma_2$. For many cases, when the lattice constant decreases the widths of the valence and conduction bands increase, as introduced by Bernal [16]. So, we notice that the state Γ_1 decreases with the increase of the compressive stress and this causes increasing in the valence band width. On the other hand, it is expected that the conduction band width increases with the increase of the compressive stress due to the increase in the state X_{ϵ_c} . But we know that the state Γ_2 moves up too. Therefore, at given compressive stress the change in Γ_2 is larger than that for X_{ϵ_c} , this makes the conduction band width ($\sim X_{\epsilon_c} - \Gamma_2$) decreases with the compressive stress. The reverse is true with the effect of tensile stress and temperature, Γ_1 moves up, this leads to decrease the valence band width. Γ_2 moves down more than that for X_{ϵ_c} , this leads to increasing the conduction band width.

4.1.6 Hybrid Crystal Orbitals

Both INDO and correlation correction give an increase in the s state occupancy, Abdul Sattar, 1997 [13] found the same effect by using INDO and correlation correction for C, Si and Ge. On the other hand, we found that when the lattice constant decreases by the effect of compressive stress, s state occupation decreases. The pressure dependence of the s state occupancy shows that electrons under pressure leave low orbitals (s orbitals) and occupy high orbitals (p orbitals). This phenomenon is known and leads to phase transitions due to the change of electronic distribution such as the s-d transition in alkali Metals [90]. So, we expect that the electrons change their positions at half the distance between two neighboring atoms. In the case of the effect of temperature and tensile stress the s state occupation increases because increasing the distance between atoms, this reflect the tendency of atoms to return their atomic configuration s^2p^2 .

4.1.7 The Bulk Modulus

The calculated value of bulk modulus is higher than the experimental value. Furthermore, we have calculated the bulk modulus without using the correlation correction because this correction leads to very high value of bulk modulus. So we expect that the correlation correction does not always lead to an enhancement in the calculated values. We think that the deviation in the value of bulk modulus, especially when we use the correlation corrections, comes from the choosing of the parameters ζ and β . In the choosing of these parameters, we have desired the enhancement of the band structure of the crystal. In the same time the best parameters set that may be preferred to band structure and some properties may cause deviation in the other properties. Therefore, the error in bulk modulus may be higher as we use

the correlation correction. Furthermore, we notice that the correlation correction causes meanders in the curves of the properties when they are as functions of lattice constant. M.A. Abdul Sattar [13] has found that the parameter ζ has higher effect on the bulk modulus than the parameter β^0 for silicon crystal. This confirms that the calculated value depends on the choosing of these two parameters.

4.1.4 Valence Charge Distribution

The valence charge density is determined from the density matrix. The charge is accumulated along the distance between the atoms. We can also notice that the overall electron cloud in the region between two atoms decreases and is compensated by an increase in the spherical charge distribution around the atoms as the lattice constant increases by temperature or tensile stress. This can be expected from the hybridized crystal states that show an increment in the s state occupancy which is of a spherical shape. The reverse of this case may be expected with the compressive stress, in spite of that the decreasing of s state occupancy and increasing the p state occupancy are not shown obviously in their figures due to the very small changes in the occupancy of the s and p orbitals. On the other hand, the computed charge distribution is not too much affected by INDO and correlation correction. The effect of these corrections is to transform some of the electronic charge from the region of the bands to the spherical region around the atoms.

4.1.9 X-Ray Scattering Factors

The calculated x-ray scattering factors are in good agreement with the experimental values. We have got this agreement because we have added the electronic charge densities of the core [ρ_c] to the valence charge density of the crystal. The previous Hartree-Fock calculations have good results because they have included core states. On the other hand, we note that the x-ray scattering factors decrease with the increase of the compressive stress. We think that when the compressive stress increases, the electronic charge distribution decreases in the near distances from the center of atoms. thus we show a decrease of the s state occupation with the increasing of the compressive stress. Therefore, the result of $\rho_c(r) \exp(-iG \cdot r)$ decreases, and it increases with tensile stress or temperature because of the increasing of s state occupation. On the other hand, there are many results of form factors of different elements which have been calculated as a function of $\sin \theta / \lambda$ where θ is x-ray incident angle and λ is the wavelength of the x-ray radiation [3, 13]. When the factor $\sin \theta / \lambda$ increases the form factors decrease. So, according to Bragg condition $n\lambda = 2d \sin \theta$ where d is the distance between two parallel planes, the factor $\sin \theta / \lambda$ is directly proportional to $1/d$. When the compressive stress increases the distance (d) will decrease because of the decreasing in the lattice constant. Therefore, the form factors decrease. The reverse is true in the cases of tensile stress and temperature.

4.2 Conclusions

1. The values of the empirical parameters $\frac{1}{2}(I_s + A_s)$ and $\frac{1}{2}(I_p + A_p)$ of the solid have different values from that of the atom.
2. The absolute value of the bonding parameters β^o for the solid is less than that for the molecule because of the high number of bond in solid.
3. The value of the orbit exponent (ζ) determines the charge distribution in the solid. The value of this parameter is larger than that for the atom, because it indicates the contracted charge distribution for solid and the diffuse charge distribution for atom.
4. The calculated value of the cohesive energy found by INDO and correlation correction is approximately equal to the experimental value. These corrections give better result for the cohesive energy than the result of CNDO.
5. The absolute value of cohesive energy decreases as the compressive stress or tensile stress or temperature increases. The cohesive energy is a function of the total energy and the total energy has a high sensitive to the potential energy of the crystal. The potential energy of the crystal varies with all the aforementioned effects. This leads to a decrease in the absolute value of the total energy and hence a decrease in the absolute value of the cohesive energy.
6. The calculated value of the direct band gap is greater than the experimental value. This can be attributed to the neglecting of the state of the core and using ζ and β^o to be equal for s and p wavefunction. The direct band gap increases as the compressive

CHAPTER 4. DISCUSSION, CONCLUSIONS AND SUGGESTIONS

stress increases and decreases with the increase of the tensile stress or temperature.

٧. The valence band width increases with increasing the compressive stress. The state Γ_1 moves down as the compressive stress increases and leads to increasing the valence band width. On the other hand, the conduction band width in this case decreases because the state Γ_2 moves up more than the state X_{ζ_c} . The reverse of these situations happens with the tensile stress or temperature because the states Γ_1 , Γ_2 and X_{ζ_c} move in the opposite directions.
٨. The s state occupation decreases with increasing the compressive stress.. When the lattice constant increases by the effect of the tensile stress or temperature the s state occupation increases. This reflects the tendency of the atom to retain their atomic configuration $s^1 p^1$.
٩. The calculated value of the bulk modulus is larger than the experimental value. The parameters ζ and β^o and the correlation correction have high effect on the calculated value of the bulk modulus.
١٠. From the valence electronic charge distribution, it is noted that the electronic charge density is high at the half distance between two atoms, and it has a small variation with the pressure or temperature.
١١. The form factors are in good agreement with the experimental results. The form factors decrease as the compressive stress increases and their values increase with increasing the tensile stress and temperature.

CHAPTER 4. DISCUSSION, CONCLUSIONS AND SUGGESTIONS

12. The tensile stress and temperature have the same effect on the properties because they increase the lattice constant of the crystal.
13. We expect that our calculations for the effect of temperature are not always of good precision because these calculations do not include the electron-phonon interaction.
14. In spite of the large number of approximations in the adopted model, the optimum empirical parameters give results in good agreement with the experimental results.

4.3 Suggestions

We suggest:

1. Applying the present work calculations to a larger LUC of 16, 64 or 128 LUCs to investigate the band structure, optical properties and effective masses. This will lead to a more detailed band structure due to the large number of symmetry points that will be produced, and it is expected that will give more precise results .
2. Applying other methods of approximations such as modified intermediate neglect of differential overlap (MINDO) or the neglect of the diatomic differential overlap (NDDO) for computing the two-electron integrals. But these levels of approximations need advanced computers and much greater computing time.
3. Using the present model with the different LUCs to study the phase transitions in tin and in other semiconductor such as Si and Ge.
4. Study of the effect of temperature on the properties of tin or other semiconductors by considering the vibrational contribution to the free energy.

CHAPTER 4. DISCUSSION, CONCLUSIONS AND SUGGESTIONS

- . Study of the effect of pressure on different semiconductors by using other methods of approach in quantum mechanics such as density-functional theory (DFT) calculations.
- ∩. Applying the present work to study the properties of the ionic crystals and the superconductive copper oxide crystalline compounds.
- ∪. Study the effect of pressure on some molecules by using ab-initio calculations.

Index of Widely Used and Important Symbols

λ - Alphabetical Symbols	
a	Lattice constant
A_{μ}	Affinity
B	Bulk modulus
$C_{\mu i}$	Combination coefficients of hybridized orbitals
E^T	Total energy
$E^{(0)}$	The zero-order energy
$E^{(1)}$	The first-order energy correction
$E^{(2)}$	The second-order energy correction
f	X-ray form factor
f(x)	Modulating function
$F_{\mu\nu}$	Fock Hamiltonian matrix element between orbitals μ and ν
F'	Zero order two-electron integral
F''	Second order two-electron integral
G'	First order two-electron integral
H^T	Total Hamiltonian operator

Appendix A

The Overlap Integrals and Slater Integrals

To evaluate the overlap integrals, the prolate spheroidal coordinate system (μ, ν, ϕ) is used.

The relations between the prolate spheroidal system and two spherical polar systems centered at atoms A and B separated by a distance R are [5],

$$\mu = \frac{r_A + r_B}{R}, \nu = \frac{r_A - r_B}{R} \quad (\text{A.1})$$

$$r_A = \frac{R(\mu + \nu)}{2}, r_B = \frac{R(\mu - \nu)}{2} \quad (\text{A.2})$$

The product of the spherical harmonic functions centered on a and b in terms of a function of prolate spheroidal coordinates $T(\mu, \nu)$.

$$T(\mu, \nu) = \theta_{l_a}^m(\cos\theta_A) \theta_{l_b}^m(\cos\theta_B) \quad (\text{A.3})$$

Where l_a and l_b are the angular quantum numbers for a and b respectively and

$$\cos\theta_A = \frac{1 + \mu\nu}{\mu + \nu} \quad \cos\theta_B = \frac{1 - \mu\nu}{\mu - \nu} \quad (\text{A.4})$$

The final form of $T(\mu, \nu)$ can be written as

Appendix B

Two-Center and One-Center Coulomb Integrals in INDO Approximation

Two center electron-electron interaction integrals of the coulomb type over Slater s functions have the following form

$$\gamma(n_a, n_b, \zeta_a, \zeta_b, \mathbf{R}) = \int \int \Omega_{aa}(1) r_{12}^{-1} \Omega_{bb}(2) d\tau_1 d\tau_2 \quad (\text{B.1})$$

Where the charge distribution $\Omega_{aa}(1)$ and $\Omega_{bb}(2)$ are the product of Slater s function. The two-center integrals are developed for programming in its final form. These integrals can be calculated using the formula of the reduced overlap integrals [3],

$$\begin{aligned} \gamma(n_a, n_b, \zeta_a, \zeta_b, \mathbf{R}) = & \frac{(2\zeta_a)^{2n_a+1}}{(2n_a)!} \left[\left(\frac{\mathbf{R}}{2} \right)^{2n_a} s(2n_a - 1, 0, 0, 0, 0, 2\zeta_a \mathbf{R}, 0) \right. \\ & - \sum_{l=1}^{2n_b} \frac{l(2\zeta_b)^{2n_b-l}}{(2n_b-l)! 2n_b} \left(\frac{\mathbf{R}}{2} \right)^{2n_b-l+2n_a} \\ & \left. \times s(2n_a - 1, 0, 0, 2n_b - l, 0, 2\zeta_a \mathbf{R}, 2\zeta_b \mathbf{R}) \right] \quad (\text{B.2}) \end{aligned}$$

and the integrals are programmed in this form in the present work. On the other hand, a general expression for one-center coulomb integrals over Slater s functions is given by

$$\gamma(n_a, n_b, \zeta_a, \zeta_b, 0) = \int \Omega_{aa}(1) \int r_{>}^{-1} \Omega_{bb}(2) d\tau_1 d\tau_2 \quad (\text{B.3})$$

And finally the form of this integrals can be written by using the reduced overlap integral as follows,

LIST OF SYMBOLS

H_e	Electronic Hamiltonian operator
H_{ii}	Expectation value of core Hamiltonian
H^{core}	Core Hamiltonian
H'	Correlation correction core Hamiltonian
I_μ	Ionization potential
J_{ij}	Coulomb integral
J_j	Coulomb operator
K_{ij}	Exchange integral
K_j	Exchange operator
k	Wave vector
P	Pressure
$P_{\mu\nu}$	Density matrix
Q_B	Net charge on atom B
r	Radial distance
r_{12}	Distance between particle one and two
s	Reduced overlap integral
S	Overlap integral
T	Temperature

LIST OF SYMBOLS

$U_{\mu\mu}$	Local core matrix element
V	Volume
V_p	Potential
V_{AB}	The interaction potential of valence electron on atom A with the core of atom B
X	High symmetry points in k space
Y_{lm}	Spherical harmonics
Z	Nuclear charge
Υ - Greek symbols	
α_L	Linear thermal expansion coefficient
β°	Bonding parameter
γ_{AB}	Two-electron integral between atoms A and B
Γ	High symmetry point in k space
$\delta_{\mu\nu}$	Kronecker delta
ε	Eigen values of Fock Hamiltonian
ζ	Orbital exponent
$(\mu\nu / \lambda\delta)$	Two-electron integral
ρ_c	Electronic charge density

LIST OF SYMBOLS

ϕ_i	Atomic wavefunctions
$X(k,r)$	Molecular wavefunction within one LUC
ψ_i	Hybridized orbital
Ψ	Total anti symmetric wavefunction
ζ - Abbreviations	
bcc	Body centered cubic
bct	Body centered tetragonal
CI	Configuration interaction
CNDO	Complete neglect of differential overlap
fcc	Face centered cubic
GTO	Gaussian type orbital
HF	Hartree Fock
INDO	Intermediate neglect of differential overlap
LCAO	Linear combination of atomic orbitals
LUC	Large unit cell
MINDO	Modified intermediate neglect of differential overlap
MPPT	Møller-Plesset perturbation theory
NDDO	Neglect of diatomic differential overlap

LIST OF SYMBOLS

sc	Simple cubic
SCF	Self-consistent field
STO	Slater type orbital
TBM	Tight-binding method
ZDO	Zero differential overlap

REFERENCES

References

١. J.L. Powell and B. Crasemann, "Quantum mechanics", Addison Wesley Publishing Company. Inc., (١٩٦١).
٢. J.A. Pople and D.L. Beveridge, "Approximate molecular orbital theory", Mc Graw-Hill, (١٩٧٠).
٣. C. Kittel, "Introduction to solid state physics", John Wiley & Sons, (١٩٩٦).
٤. J.S. Blakemore, "Solid state physics", Cambridge University Press, (١٩٧٤).
٥. H.P. Myers, "Introductory solid state physics", Taylor & Francis, (١٩٩٠).
٦. W.J. Moore, "Physical chemistry", Longmans, Green and Co, (١٩٥٧).
٧. S.M. Sze, "Semiconductor devices: physics and technology, translated to Arabic by F.G. Hayaty and H.A. Ahmed, Dar Al-HiKma-Mosul, (١٩٩٠).
٨. R.T. Morrison and R.N. Boyd, "Organic chemistry", Allyn and Bacon, Inc., (١٩٨٧).
٩. Manas Chanda, "Atomic structure and chemical bond", Mc Graw-Hill, (١٩٧٩).
١٠. J. Burdett, "Chemical bonds", John Wiley and Sons, (١٩٩٧).
١١. E. Kaxiras, "Atomic and electronic structure of solids", Cambridge University Press, (٢٠٠٣).
١٢. F. Bassani, G.P. Parravicini and R.A. Ballinger, "Electronic states and optical transitions in solids", Pergamon Press, (١٩٧٥).

REFERENCES

١٣. M.A. Abdul Sattar, "Self-consistent field calculations of covalent semiconductors, Ph. D. thesis, University of Baghdad, (١٩٩٧).
١٤. A. Svane, Phys. Rev. B, V ٣٥ P ٥٤٩٦ (١٩٨٧).
١٥. J.E. Szymanski, "Semi-empirical methods of total energy calculations", Ph. D. thesis, University of York, (١٩٨٤).
١٦. B. Akdim, D.A. Papaconstantopoulos and M.J. Mehl, Philosophical Magazine B, V ٨٢ P ٤٧ (٢٠٠٢).
١٧. N. Moll, M. Bockstedte, M. Fuchs, E. Pehlke and M. Scheffler, Phys. Rev. B, V ٥٢ P ٢٥٥٠ (١٩٩٥).
١٨. B. Westrum and Y. Tbmassen, "Tin and inorganic tin compounds", National institute for working life, (٢٠٠٢).
١٩. A.T. Khn, P.R. Berger, F.J. Guarin and S.S. Lyer, Appl. Phys. Lett, V ٦٨ P ٣١٠٥ (١٩٩٦).
٢٠. H. Perez Ladron de Guevara, H. Navarro-Contreras and M.A. Vidal, Superficies y Vacio ١٦(٤) P٢٢ (٢٠٠٣).
٢١. A. Mujica, Angel Rubio, A. Mvnoz and R.J. Needs, Rev. Mod. Phys., V ٧٥ P ٨٦٣ (٢٠٠٣).
٢٢. F. Bassani and L. Liu, Phys. Rev., V ١٣٢ P ٢٠٤٧ (١٩٦٣).
٢٣. F.H. Pollak, M. Cardona, C.W. Higginbotham, F. Herman and J.P. Van Dyke, Phys. Rev. B, V ٢ P ٣٥٢ (١٩٧٠).
٢٤. C.J. Buchenauer, M. Cardona and F.H. Pollak, Phys. Rev. B, V ٣ P ١٢٤٣ (١٩٧١).
٢٥. A.H. Harker and F.P. Larkins, J. Phys. C, V ١٢ P ٢٤٩٧ (١٩٧٩).
٢٦. PE. Van Camp, V.E. Van Doren and J.T. Devreese, Phys. Rev. B, V ٣٨ P ١٢٦٧٥ (١٩٨٨).

REFERENCES

27. P. Pavone, S. Baroni and S. de Gironcoli, Phys. Rev. B, V 67 P 10421 (1998).
28. J. Xie, S.P. Chen, J.S. Tse, S. de Gironcoli and S. Baroni, Phys. Rev. B, V 60 P 9444 (1999).
29. P. Pavone, J. Phys: Condens. Matter 13 P 7093 (2001).
30. R. Asokamani and R. Rita, Phys. Stat. Sol. (b), V 226 P 370 (2001).
31. D. Olguin, A. Contarero, C. Ulrich and K. Syassen, Phys. Stat. Sol. (b), V 230 P 406 (2003).
32. P.T. Matthews, "Introduction to quantum mechanics", Mc Graw-Hill, (1974).
33. V.A. Fock, "Fundamentals of quantum mechanics", Mir Publishers, (1978).
34. M.W. Hanna, "Quantum mechanics in chemistry", W.A. Benjamin, Inc., (1979).
35. P. Norman and L. Ojamae, "Laborations in quantum chemistry", University of Linkoping, (2004).
36. G. Hunter, "Quantum Chemistry: Wave mechanics applied to atoms and molecules" www.yorku.ca/ghunter/eq-root.pdf, (2001).
37. Yao Cong, "Introduction to quantum chemistry", <http://biomacina.org/courses/modeling/12.html>.
38. C. David Sherrill, "A brief review of elementary quantum chemistry", Georgia Institute of Technology, (1997).
39. E.F. Valeev and C.D. Sherrill, J. Chem. Phys. V 118 P 3921, (2003).

REFERENCES

٤٠. P.W. Atkins and R.S. Friedman, "Molecular quantum mechanics", Oxford University Press, (١٩٩٧).
٤١. E.U. Condon and H. Odishaw, "Handbook of physics", Mc Graw-Hill, (١٩٦٧).
٤٢. P. Cronstrand, "Quantum chemical calculations of nonlinear optical absorption", Stockholm, (٢٠٠٤).
٤٣. J.P. Goss, "A first principles study of defects in semiconductors", Ph. D. thesis, University of Exeter, (١٩٩٧).
٤٤. B.H. Bransden and C.J. Johchain, "Physics of atom and molecules", Lohgman, (١٩٨٣).
٤٥. Per-Erk Larsson, "Modelling chemical reactions", Acta Universitatis Upsaliensis Uppsala (٢٠٠٣).
٤٦. J.R. Chelikowsky and Y. Saad, "Electronic structure of clusters and nano crystals", University of Minnesota, (٢٠٠٤).
٤٧. P.W. Atkins, "Physical chemistry", Oxford University Press, (١٩٩٨).
٤٨. W. Hehre, L. Radom, P. Schileyer and J. Pople, "Ab-initio molecular orbital theory", John Wiely and Sons, (١٩٨٦).
٤٩. M. Troyer, "Computational physics II", ETH Zurich, SS (٢٠٠٣).
٥٠. Shane McCarthy, "Calculation of the electronic structure of N-electron quantum dots using the Hartree-Fock method", B.Sc. thesis, University of Western Australia (٢٠٠٠).
٥١. I.Z.A. Hassan, "Semi empirical self-consistent filed calculations of III-V Zinc-Blende semiconductors", Ph. D. thesis, University of Al-Nahrain, (٢٠٠١).

REFERENCES

٥٢. H.A. Kassim and D.A. Al-Mukhtar, "Introduction to quantum mechanics, Dar Al-Kutob, AL-Mousel University, (١٩٨٧). (in Arabic).
٥٣. R. Daudel, G. Leroy, D. Peeters and M. Sana, "Quantum chemistry", John Wiley and Sons, (١٩٨٣).
٥٤. P. Chen, "Qualitative MO Theory and its application to organic reactions, thermal rearrangements, pericyclic reactions", ETH Zurich, SS (٢٠٠٥).
٥٥. J. Simons, "An introduction to theoretical chemistry", Cambridge University Press, (٢٠٠٣).
٥٦. D. Marx and J. Hutter, "Ab initio molecular dynamics: Theory implementation", John Von Neumann Institute for Computing, (٢٠٠٠).
٥٧. H. Dorsett and A. White, "Overview of molecular modelling and ab initio molecular orbital method suitable for use with energetic materials", Defence Science and Technology Organisation, (٢٠٠٠).
٥٨. W. Thiel, "Semi-empirical methods", John Von Neumann institute for computing, (٢٠٠٠).
٥٩. J. Pople, D. Santry and G. Segal, J. Chem. Phys., V ٤٣ P S١٢٩ (١٩٦٥).
٦٠. J. Pople and G. Segal, J. Chem. Phys., V ٤٣ P S١٣٦ (١٩٦٥).
٦١. J. Pople *et al.* J. Chem. Phys., V ٤٧ P ٢٠٢٦ (١٩٦٥).
٦٢. J. Slater, "Quantum theory of atomic structure", V ١ P ٣٣٩-٣٤٢ Mc Graw-Hill, (١٩٧٤).
٦٣. A. Harker and F. Larkins, J. Phys. C, V ١٢ P ٢٤٨٧ (١٩٧٩).

REFERENCES

٦٤. C. Nayak, "Solid state physics", University of California, (٢٠٠٠).
٦٥. R. Evarestov and V. Smirnov, Phys. Stat. Solidi (b), V ١١٩ P ٩ (١٩٨٣).
٦٦. C.D. Sherrill, "An introduction to configuration interaction theory", Georgia Institute of Technology, (١٩٩٥).
٦٧. C. David Sherrill, "Derivations of the configuration interaction singles method for various single determinant references and extensions to include selected double substitutions", Georgia Institute of Technology, (١٩٩٦).
٦٨. R. Ahlrichs, S. Elliot and U. Huniar, "Ab initio treatment of large molecules", John Von Neumann Institute for Computing, (٢٠٠٠).
٦٩. P. Knowles, M. Schutz and Hans-Joachim Werner, "Ab initio methods for Electron correlation in molecules", John Von Neumann Institute for Computing, (٢٠٠٠).
٧٠. J.L. Calais E. Kryachko, "Conceptual perspectives in quantum chemistry", Kluwer Academic Publishers, (١٩٩٧).
٧١. K. Schwarz and P. Blaha, "Quantum mechanical computations at the atomic scale for material sciences", Fifth World Congress on Computational Mechanics, (٢٠٠٢).
٧٢. J.J. Rehr and R.C. Albers, Rev. Mod. Phys., V ٧٢ P ٦٢١ (٢٠٠٠).
٧٣. K. Balasvbramanian, "Relativistic effective core potential techniques for molecules containing very heavy atoms, Wiley-Inter-Science, New York, (١٩٩٨).
٧٤. M. Reiher and B. Heb, "Relativistic electronic-structure calculations for atoms and molecules, John Von Neumann Institute for Computing, (٢٠٠٠).

REFERENCES

٧٥. D. Chadi, Phys. Rev. B, V ١٦ P ٧٩٠ (١٩٧٧).
٧٦. C. Allen, "Astrophysical Quantities", Athlone press, (١٩٧٦).
٧٧. W. Lambrecht and O. Anderson, Phys. Rev. B, V ٣٤ P ٢٤٣٩ (١٩٨٦).
٧٨. Zahlenwerte und funktionen aus Naturwissenschaften und Technik, N. S. Vol. III ١٧a of Landölt-Börnstein, edited by O. Madelung (Springer, New York, ١٩٨٢).
٧٩. O. Madelung (editor), "Zahlenwerte and Funktionen aus naturwissenschaften and technik, "V ١١١", Springer (١٩٨٢).
٨٠. Private communication with Dr. N. Rammo, University of Baghdad.
٨١. D. Cromer and J. Mann, Acta Cryst., V A٢٤ P ٣٢١ (١٩٦٨).
٨٢. F. Bueclte, "Principle of physics", Mc Graw-Hill, (١٩٨٢).
٨٣. Y.S. Touloukian, R.K. Kirby, R.E. Taylor and P.D. Desai, Thermophysical properties of matter, V ١٢ (١٩٧٥).
٨٤. Material Property Database (MPDB), Jahm software, Inc., <http://www.jahm.com>, (٢٠٠٢).
٨٥. R. Boca, Int. J. Quantum Chem. V ٣١ P ٩٤١ (١٩٨٧).
٨٦. E. Clementi and C. Roetti, "Atomic and nuclear data tables", V ١٤ (١٩٧٤).
٨٧. S.K. Tewksbury, "Semiconductor materials", West Virginia University, (١٩٩٥).
٨٨. R. Pässler, Phys. Stat. Sol. (b) V ٢١٦ P ٩٧٥ (١٩٩٩).
٨٩. John N. Murrell, Sydney F.A. Kettle and J.M. Tedder, "The chemical bond", Translated to Arabic by M.N. Al-Zakum, Al-Basrah University (١٩٨٣).
٩٠. K. Takemura and K. Syassen, Phys. Rev. B, V ٢٨ P ١١٩٣ (١٩٨٣).